Experimentation, Modeling and Control of Calcium Dynamics in Human Vascular Endothelial Cells

CAO Lingling

Department of Electrical and Computer Engineering

National University of Singapore

A thesis submitted for the degree of

Doctor of Philosophy

2012

I would like to dedicate this thesis to my loving parents, for their unconditional love and support.

Acknowledgements

I would like to acknowledge:

Prof. Xiang Cheng, my supervisor, for his guidance throughout my 5 year Ph.D candidature. The research work presented in this thesis could not be accomplished without him.

Prof. Lee Tong-Heng, my co-supervisor, for his insight and encouragement throughout past 5 years.

Prof. Li Jun, our collaborator from Division of Bioengineeing, for his generous provision of necessities without which the cell experiments could never been conducted.

Prof. Qin Kai-rong, who once worked in our group, for his guidance in this project.

My friends, lab officers and teachers who have ever guided my life and study. I treasure their friendships and appreciate their long lasting concerns and supports. My Ph.D study in Singapore would be an irreplaceable experience in my future life.

Abstract

Calcium ion (Ca^{2+}), as a ubiquitous second messenger found in almost all types of cells, has played an important role regulating various cellular functions. In human vascular endothelial cells (VECs), the dynamic behavior of intracellular calcium, i.e., its temporal/spatial variation, will directly affect cell proliferation, synthesis and secretion of vaso-active factors like nitric oxide (NO), and gene regulation. Therefore finding the way to encode useful information into calcium signaling process, that is to adjust the calcium dynamics via external stimuli, has become extremely meaningful.

In this thesis, we are trying to construct the framework under which the regulation of intracellular calcium dynamics could be investigated via mathematical modeling and wet lab experimentation as well. A microfluidic device is fabricated for cell culture and flow loading tests. When VECs are settled down in the chip, buffer medium containing different levels of adenosine triphosphate (ATP) could be applied to them at different flow rates (or shear stresses). The intracellular calcium level is monitored through a fluorescent microscope simultaneously.

To achieve successful intracellular calcium regulation, it is necessary to gain a comprehensive understanding of the interplay among shear stress, ATP and calcium dynamics. The significance of quantitative analysis of the whole system is obviously seen. Based on our own experiments and those published ones, we have built three mathematical models to capture shear stress-induced ATP release from VECs. The conventional proportional-integral-differential (PID) controller is employed to modulate ATP release via simulation study. We then move on to regulate calcium dynamics by adjusting shear stress and exogenous ATP. The profile of average calcium concentration in the observation field is recorded. By feeding the system a pre-designed control command, we can generate letters “N”, “U” and “S” (representing National University of Singapore) in this profile. The feedback control is also implemented. The knowledge-based fuzzy rules are utilized to

update input signals and the experimental results indicate a better tracking of letters “N”, “U” and “S”.

Though we know very little of the downstream reactions triggered by such “N”, “U” and “S” calcium profiles, it is believed the work presented in this thesis might open up a new scenario where engineering approaches, i.e., system and control theory, could be applicable to a biological plant at cellular and/or gene level, facilitating the biochemical reactions involved toward a beneficial direction promisingly.

Contents

List of Figures

Chapter 1

Introduction

1.1 Endothelium, Mechanotransduction and Vascular Biology/Pathophysiology

1.1.1 Views of Biologists

Endothelium is a monolayer of cells lining the inner wall of blood vessel and works as a barrier separating the blood flow and vascular muscle cells. As continuously exposed to the flowing blood, vascular endothelial cells (VECs) have gradually evolved to be highly-sensitive to hemodynamic forces, like shear stress and stretch[1] for example.

A notable phenomenon has been well observed and reported as early as in the 19th century that the atherosclerotic lesions first occur in branches or curvature parts of the artery where the shear stress is usually low and the blood flow no longer laminar (Virchow [1850]). In a more recent survey in 2011, Chiu and Chien (Chiu & Chien [2011]) review the latest experimental and theoretical knowledge on VECs responses to complex flow patterns both *in vitro* and *in vivo*. They confirm the significant role of blood flow in endothelial dysfunction based on clinical observations.

Therefore endothelium is not merely a physical interface but rather a multi-functional mediator responsible for various hemodynamic-related affairs in vascular biology or pathophysiology (Davies [2009]; Hahn & Schwartz [2009]; Nerem [1992]). A large body of experimental results have shown that VECs could sense mechanical forces from the environment and respond accordingly (see Chien [2007]; Davies [1995, 1997] and references therein). The process by which mechanical signals are received by cells and con-

[1] shear stress: frictional force exerted on VECs surface per unit area and stretch: pressure generated on VECs due to pulsatile blood flow

verted into biochemical ones is termed as mechanotransduction (Ingber [1991, 2003]). Stimulated by the hemodynamic forces, sensors on the cell membrane are believed to activate the intracellular signaling pathway and initiate a chain of biochemical reactions, which affect gene and protein expressions (Ohura *et al.* [2003]; Toda *et al.* [2008]). As a consequence, VECs functions including cell migration, proliferation, apoptosis and synthesis and secretion of metabolic substances are regulated.

Most research work in this area carried out by biologists and physiologists are focused on identifying the structure of the mechano-sensor in VECs membrane, finding signaling pathway given certain type of mechanical stimulus and investigating the interplay of gene expression and cell function. Qualitative analysis takes a dominant role and the majority of findings have been established on the platform where knowledge and methodology in chemistry and molecular biology are the major components. Their reports, to some extent, read quite "uncomfortable" to engineers who have been long working with machines and tend to step into the world of mechanobiology in the very beginning. In the subsection below, another version of statement is provided from a more engineering perspective.

1.1.2 Views of Engineers

Here we would like to provide another version of explanation on what endothelial mechanotransduction is from a more engineering perspective. Take VECs as a separated system. Due to its complex nature in terms of structure and function, it is like a black box (or a plant) commonly seen in a practical engineering system. The hemodynamic forces, i.e., shear and stretch exerted on the cells are viewed as the input signal. The membrane receptors are the transducers initiating the signal relay, during which a transient response, say a sudden increase of certain molecules inside VECs is elicited. The phenomenon of interest observed from this plant, like gene expression, is the output. The principle adopted by the plant to interpret input signal to guide its operation is called mechanotransduction mechanism.

Since the mechanical-sensitive endothelium shares many aspects with common engineering system, it is very natural to think of borrowing some ideas and methods there so as to enhance our understanding of VECs behavior especially via quantitative analysis of several critical factors involved in mechanotransduction process. In this thesis, we aim to construct an engineering environment for cell growth, inject different stimuli and record corresponding cell responses. By doing so, a detailed quantitative model could be developed and human intervention for cellular events may also be achieved via

manipulating stimuli delicately. However, the primary task is to choose a well-known signaling pathway as the objective plant whose input is not too hard to generate and output signal measurable.

1.2 A Benchmark Endothelial Signaling Pathway

1.2.1 Views of biologists

Endogenous nitric oxide (NO) is a well-recognized endothelial-derived relaxing factor (EDRF) responsible for vasodilation and hence regulating blood pressure in living body (Loscalzo & Welch [1995]; Moncada & Higgs [2006]). Research work focused on NO and its role in cardiovascular system was initiated by Furchgott and Zawadzki (Rurchgott & Zawadzki [1980]) some 30 years ago, after which numerous findings have been coming up in a world wide range (da Silva *et al.* [2009]; Sessa [2005]). Many diseases associated with endothelium dysfunction are characterized by impair NO production and low activity of endothelial nitric oxide synthase (eNOS), a primary source of NO. Intracellular calcium plays a key role in eNOS activity (Dudzinski & Michel [2007]). A proposed mechanism is that free calcium ions bind to calmodulin to form the new complex Calcium/CaM, which would later bind to eNOS to promote NO release (Förstermann *et al.* [1991]; Lopez-Jaramillo *et al.* [1990]). There are also other studies (Ranjan *et al.* [1995]; Xiao *et al.* [1997]) reporting that eNOS could be activated by shear stress even without the presence of calcium. However, eNOS expression is calcium-dependent and manifests different activation level when surrounding calcium concentration varies.

What could be the upstream activator for the intracellular calcium response? Ando and his colleagues (Ando *et al.* [1988]) first discovered the cytoplasmic calcium elevation to increased shear stress in 1988. However their discovery was not immediately accepted but brought about a heated debate in early 1990s. Mo *et al* (Mo *et al.* [1991]) and Dull and Davies (Dull & Davies [1991]) demonstrated that calcium transients would occur in VECs when the perfusate contained adenosine triphosphate (ATP). The binding of ATP to P2Y receptors activated phospholipase C and then generated inositol1,4,5-phosphate ($Ins(1,4,5)P_3$), which triggered calcium release from intracellular calcium stores (Hallam & Pearson [1986]; Olsson & Pearson [1990]; Pirotton *et al.* [1987]). They believed that the flow modified the local concentration of ATP on cell surface, influencing calcium mobilization in an indirect fashion. In the meanwhile, there were several other groups providing their results supporting Ando's point of view. Shen *et al* (Shen *et al.* [1992]) observed a sharp increase of calcium in cultured VECs shortly after

the application of a step increase shear stress (0.008→0.8Pa). Geiger *et al* (Geiger *et al.* [1992]) obtained similar results and analyzed the spatial/temporal calcium dynamics from a single VEC. Helmlinger *et al* (Helmlinger *et al.* [1995]) applied pulsatile and steady flow and found different calcium responses. James *et al* (James *et al.* [1995]) utilized confocal microscopy to show that the duration of calcium response was altered by shear stress. Although calcium response induced by mere shear stress was gradually accepted, its molecular mechanism was not yet identified by mid 1990s (Malek & Izumo [1994]).

In 2000, Ando's student, Yamamoto and her colleagues first recognized the strong expression of P2X4 receptor in human VECs (Yamamoto *et al.* [2000b]). Different from P2Y receptor family whose signaling process requires the participation of G protein, P2X4 receptor is iontropic. Gated by extracellular ATP, it would directly control the flux of free calcium ion across the cell membrane (Yamamoto *et al.* [2000a]). In 2003 Yamamoto *et al* (Yamamoto *et al.* [2003]) reported that stepwise increased shear stress led to stepwise increased ATP release, which finally caused a stepwise increased calcium level in human pulmonary artery endothelial cells (HPAECs). She hypothesized that it was the endogenously released ATP, which again bond to P2X and P2Y receptors, that initiated the calcium response in HPAECs. Later in 2007, Yamamoto *et al* Yamamoto *et al.* [2007] justified her hypothesis by demonstrating the molecular mechanism of shear-stress-induced ATP release. F_1F_0ATP synthase was identified as the generator of ATP and it was activated when HPAECs were exposed to flow. It was then confirmed that mere shear stress could successfully trigger calcium dynamics in VECs as long as they possessed strong ATP release capacity.

1.2.2 Views of Engineers

By far we have a clear picture of one typical signaling pathway in human VECs. It starts from shear stress generated by blood flow and ends with the production of one significant vasorelaxation factor–NO. VECs could release ATP either via F_1F_0ATP synthase or ion channels (Sabirov & Okada [2005]) in response to shear stress. ATP in the extracellular space would then bind to P2X and P2Y receptors leading to the calcium influx from the exterior of VECs and calcium release from interior calcium stores, respectively. Free calcium ion in the cytoplasm is thus altered and being able to regulate the bioactivity level of eNOS, a physiological source of NO.

The pathway is actually a cascade system, which could be decoupled into several subsystems each with input(s) from the upstream reaction and output(s) to initiate

remote downstream reaction. The topological structure of these subsystems would largely determine the complexity of the whole system. As aforementioned, shear stress could affect eNOS activity alone, implying a coupling mechanism. NO release enhances vessel relaxation, enlarges the diameter of the lumen and consequently reduce the flow rate and shear stress as well. This is the feedback mechanism. To avoid an overcomplex structure of the plant, we only consider the first half pathway–that is shear-stress-induced calcium response in VECs– because:

- Human intervention of cell behavior is still in its infant stage and it's wiser not to make the problem too complicated.
- Information encoding and decoding is already well represented along "shear stress → ATP → intracellular calcium" pathway. Different patterns of flow are encoded in mechanical stimuli, shear stress. ATP is capable of decoding information in shear stress by manifesting different release amount accordingly. A similar encoding/decoding process is applicable to calcium response as well.
- Measurement of multiple biochemical substances in one signaling pathway will increase the difficulty in experiment and sometimes may bring unnecessary measurement error.

1.3 Thesis Objective and Outline

In this thesis, an engineering approach based on control and system theory is adopted to investigate the interplay of shear stress, ATP and calcium dynamics in human VECs. The objective is to explore whether and to what extent, if possible, intracellular calcium level could be modulated by carefully adjusting shear stress and ATP. To achieve the ultimate goal, we break the whole problem into subsections–experimentation, modeling and control of calcium dynamics–and tackle them one by one.

In Chapter 2, three mathematical models of shear-stress-induced ATP release are developed. Being the first reaction in the benchmark pathway, its dynamic feature of ATP release has attracted us in the very beginning. The amount of ATP given off by VECs would gradually decrease if hey have been exposed to a constant shear stress for a long time. This is quite different from the common sense we have gained in engineering system. The DC motor would keep working provided that power supply is sufficient. For living cells, they would adapt to the environment and become less sensible to the unchanged external stimulus. This phenomenon is called "desensitization",

which unfortunately receives little attention from engineers. In order to capture the "desensitization characteristic", we propose these three dynamic ATP releaae models. The original dynamic model could well describe the receptor desensitization. However, it lacks reactivation mechanism, implying that cells could not restore the capacity to release ATP even for a second time. We thus have a modified version, which inherits all the features from the original one and develops its own reactivation mechanism that the changing rate of shear stress would re-open the receptors. We have investigated another possible feature in the third model, that is cells have limited capacity to release ATP. If cells are exhausted by continuous stimulus, they would stay in the desensitized status no matter how the stimulus is altered. We predict the dynamics of ATP release via simulation studies under various shear stress stimulations. These numerical results could help us rank the performance of these models when we have produced our own experimental data, as would be elaborated in Chapter 3.

In order to determine which one of the three models could outperform the other two, we conduct the cell experiments in a polydimethylsiloxane (PDMS)-based flow chamber, named as perfusion/flow system since (1) it can be used for cell culture by perfusing fresh medium and (2) flow loading tests could be carried out on it later. The fabrication of such a device requires chamber design, mold manufacture, PDMS curing and device assembly. Photolithography technique is utilized to imprint the design on a silicon wafer as the size of the patterns are about hundred microns. The detailed procedure could be found in Chapter 3. With the perfusion/flow system, we start to develop the protocol for VECs culture in it. The growth records of VECs have shown cells could proliferate at a fast rate with the supplementation of fresh medium in our system. Their morphology is just like that in cultured in conventional flasks. We then conduct flow loading test to measure the ATP release level by applying time-variant shear stress. Our experimental results validate the hypothesis we have proposed in Chapter 2 that the changing rate of shear stress could reactivate receptors for ATP release. However cells could restore for a short time, indicating they would get exhausted.

We have attempted to modulate ATP release from VECs by adjusting the magnitude of shear stress in Chapter 4. As the release process in the chamber is governed by the diffusion and convection equation, the conventional proportional-integral-differential (PID) controller is selected to generate input signals. We have conducted simulation studies and investigate whether ATP release is controllable. The results show that the profile of the average ATP concentration at VECs surface could track some simple references such as square wave and sinusoid.

We finally move to the regulation of intracellular calcium level by adjusting both

shear stress and exogenous APT, which is also the ultimate goal of the work presented in this thesis. A flow circuit comprising the perfusion/flow system, two programmable syringe pumps, a fluorescence microscope, a camera and a PC with LabVIEW installed is first constructed. Excited by the light at certain wavelength, free calcium ion in the cell would give off fluorescence, which is then captured by the camera. The picture would send to PC for analysis and the control signal (the infusion of different levels of ATP at different rates) is thus generated according to a fuzzy rule. To orchestrate a successful operation of the circuit, we culture human pulmonary artery endothelial cells (HPAECs) in the perfusion/flow system and apply shear stress alone to test calcium signal. When the crucial parameters of the setting up have been optimized, both open loop and closed loop control schemes are implemented to the real plant. According to our observation, the average calcium level could follow some basic patterns, like spike and sigmoid. The three letters "N", "U" and "S", representing National University of Singapore, are also produced via both open loop and closed loop control. Experimental results on calcium imaging are summarized in Chapter 5.

Chapter 6 concludes the whole thesis, summarizes the main contribution and proposes several issues worth further investigation.

Chapter 2

Mathematical Modeling on Shear-stress-induced ATP Release from Human VECs

ATP release from VECs is almost a simultaneous response when shear stress is applied. The released ATP then diffuses and convects in the flowing perfusate. It is crucial to determine the ATP concentration on cell surface because intracellular calcium response is triggered by ATP binding to cell membrane receptors. In this chapter, we have developed three types of ATP release model to capture its distribution in the extracellular space. Receptor desensitization is considered in these models while three different activation mechanisms are proposed individually. Some interesting responses of the VECs are observed through simulation studies when shear stress varies in a more complex fashion against time.

2.1 Mathematical Model of ATP Release: A Quick Review

For the modulation of extracellular ATP concentration in the endothelial cell surface by fluid shear stress, much research has been conducted by a number of leading researchers. The research was first investigated in early 1990s by Nollert *et al* (Nollert & McIntire [1992]; Nollert *et al.* [1991]) and Shen *et al* (Shen *et al.* [1993]). It was suggested that convection-diffusion and ATP hydrolysis alter the distributions of extracellular ATP concentrations in the perfusate, and fluid shear stress indirectly modulates the

extracellular ATP concentrations at endothelial surface. Accordingly, their mathematical models only considered the effects of convection-diffusion and ATP hydrolysis by ecto-ATPase. In more recent pursuit, further investigations revealed that, in addition to convection-diffusion effects and ATP hydrolysis, fluid shear stress also directly induces ATP release from VECs, and the endogenously released ATP mediates the ATP concentrations in the endothelial cell surface (David [2003]; John & Barakat [2001]; Yamamoto *et al.* [2003]).

In the pioneering work of John and Barakat (John & Barakat [2001]), a static model was developed to describe the relationship between the shear stress and ATP release from endothelial cells. It was assumed that ATP release rate is either a linear or a nonlinear function of the magnitude of shear stress in the range of $0 \rightarrow 1Pa$. Their linear model takes the form of

$$S(\tau_w) = S_{\max} \cdot \tau_w, \tag{2.1}$$

where $S(\tau_w)$ is the ATP release rate induced by the shear stress of τ_w, and $S_{\max}$ is the maximum of ATP release rate. Their nonlinear model is expressed by

$$S(\tau_w) = S_{\max}\left[1 - \exp\left(-\frac{\tau_w}{\tau_0}\right)\right]^3, \tag{2.2}$$

where τ_0 is a reference shear stress. Different values of τ_0, such as $0.01, 0.1, 1$Pa, represent "rapid", "intermediate", and "slow" sigmoidal ATP release. Although their models captured a number of important features of the shear stress induced ATP release process and have been widely applied in the modeling of calcium dynamics in VECs (Comerford *et al.* [2006]; Plank *et al.* [2006]) the static models have to be modified to characterize the dynamic relationship between the shear stress and the ATP release, which is evident in the experimental studies (Guyot & Hanrahan [2002]; Yamamoto *et al.* [2003]). In particular, it was clearly shown in the experimental observations made by Yamamoto and her colleagues Yamamoto *et al.* [2003] that after shear stress is applied on ECs, shear stress induced ATP release rate will increase to reach a maximum, then decrease with time, which obviously indicates that ATP release rate should be a function of not only the magnitude of shear stress but also of the time. Hence, the relationship between the ATP release rate and shear stress should be described by a dynamic model instead of a static one.

In the following sections, we are to develop a dynamic model which is complex enough to capture the time-dependency of shear stress induced ATP release rate, and

make the modeling results more consistent with the experimental observations.

2.2 Original Dynamic ATP Release Model

2.2.1 Model Development

Before the mathematical details of the model are presented, the following definitions are in order for the convenience of discussion and presentation.

Definition 1. *A dynamic model is a mathematical description which describes the time dependence of the variables of interest, either in differential or difference equations.*

Definition 2. *A static model is a mathematical description which describes the direct and instantaneous relationships of the variables of interest, either in linear or nonlinear functions.*

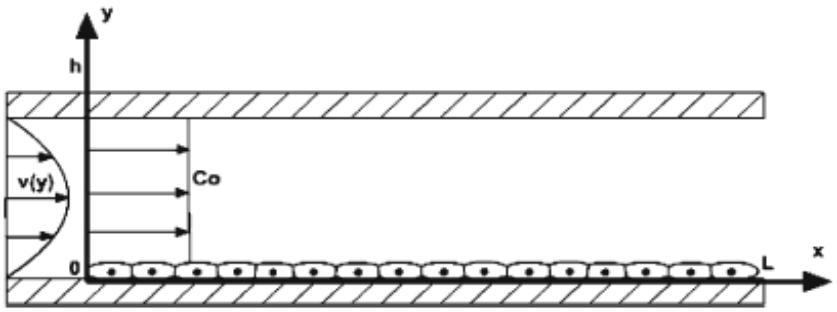

Figure 2.1: Schematic diagram of a parallel-plate flow chamber

A parallel-plate flow chamber is chosen in our simulation studies as the apparatus to apply shear stress on the VECs which are cultured on the bottom plate as shown in Fig 2.1. Prior to the onset of flow, the fluid within the flow chamber is assumed to contain ATP-free buffer medium. The initial ATP concentration in the flow chamber is assumed to be zero in all the simulations. With the activation of flow, endogenously released ATP will convect and diffuse, which may be described by the standard convection and diffusion equation,

$$\frac{\partial c}{\partial t} + v(y)\frac{\partial c}{\partial x} = D\left(\frac{\partial^2 c}{\partial x^2} + \frac{\partial^2 c}{\partial y^2}\right), \tag{2.3}$$

where c is the ATP concentration, D is the diffusion coefficient of ATP in the fluid, and $v(y)$ is the flow velocity of the perfusate. The above equation is used to describe the ATP distribution in the chamber at any specified time instance. The ATP level

at a particular point in the chamber would vary against time due to the diffusion and convection of ATP, as indicated by the two terms in Eq 2.3.

For steady flow, the velocity profile within the chamber can be obtained analytically and is expressed by *Poiseuille* formula as

$$v(y) = 6\bar{v}\frac{y}{h}\left(1 - \frac{y}{h}\right), \tag{2.4}$$

where $\bar{v}$ is the average velocity in the x direction. The shear stress to which the VECs are exposed in steady flow can then be determined directly from this profile as

$$\tau_w = \mu\frac{\partial v}{\partial y}\mid_{y=0} = \frac{6\mu\bar{v}}{h}, \tag{2.5}$$

where τ_w is the wall shear stress and μ is the dynamic viscosity of the fluid.

For the pulsatile flow, the velocity profile within the chamber can also be derived analytically. In consideration that the Womersley number $\alpha = h\sqrt{\frac{\rho\omega}{\mu}}$, where ρ is fluid density and $\omega = 2\pi f$ is the angular frequency, is normally low in the experiments, the quasi-steady flow assumption can be adopted. Following the previous studies (John & Barakat [2001]), it is assumed that the flow is purely sinusoidal such that the velocity profile is given as

$$v(y) = 6\bar{v}\frac{y}{h}\left(1 - \frac{y}{h}\right)(1 + \sin\omega t). \tag{2.6}$$

Therefore, the shear stress to which the ECs are exposed in pulsatile flow is that given in Eq.(2.5) multiplied by the sinusoidal term $(1 + \sin\omega t)$ in Eq.(2.6).

It can be readily shown by order of magnitude analysis that $\frac{\partial^2 c}{\partial x^2} \ll \frac{\partial^2 c}{\partial y^2}$, thus the term $\frac{\partial^2 c}{\partial x^2}$ can be ignored in Eq.(2.3), and diffusion is assumed to occur only in the y direction.

At time $t = 0$, since the chamber has not yet been perfused by the flow, the ATP concentration is assumed to be zero in the flow chamber, i.e.,

$$c\mid_{t=0} = 0. \tag{2.7}$$

At the entrance of the flow chamber ($x = 0$), the ATP concentration is assumed to be zero since the inflowing perfusate used in this study is fresh without any ATP.

At the upper plate of flow chamber ($y = h$), the flux of ATP is zero, i.e., the concentration gradient of ATP is zero, expressed as

$$\frac{\partial c}{\partial y}\mid_{y=h} = 0. \tag{2.8}$$

At the bottom of the flow chamber ($y = 0$), the net ATP mass flux is determined by the rate of ATP hydrolysis by ecto-ATPases on the cell surface and the rate of shear stress induced ATP release by the VECs. Similar to the previous studies (John & Barakat [2001]), it is assumed that the kinetics of ATP hydrolysis is described by an irreversible Michaelis-Menten formulation, while ATP release due to shear stress is included as a separate source term. Thus ATP flux at the VECs surface is given as

$$D\frac{\partial c}{\partial y}\mid_{y=0} = \frac{V_{\max} c}{K_{\mathrm{m}} + c}\mid_{y=0} - S_{\mathrm{ATP}}(\tau_w, t) \equiv -S_{\mathrm{net,ATP}}, \tag{2.9}$$

where D is the diffusion coefficient for ATP in the cell culture medium, $V_{\max}$ is the maximum enzyme reaction velocity for ATP hydrolysis, K_{m} is the Michaelis constant for the enzyme, $S_{\mathrm{ATP}}(\tau_w, t)$ is the source term for endothelial shear stress induced ATP release which depends upon not only the wall shear stress, τ_w, but also the time t. The average net ATP release rate $S_{\mathrm{net,ATP}}$ against time t under different wall shear stresses can be measured by *in vitro* cell experiments (Yamamoto *et al.* [2003]).

Remark 1. *As mentioned in the beginning of this chapter, the shear stress induced ATP release rate $S_{\mathrm{ATP}}(\tau_w, t)$ was assumed to be a time-independent function of only the shear stress, τ_w, in all the previous modeling analysis (David [2003]; John & Barakat [2001]), which does not match the experimental observations well. This is the first time that such a dynamic model is proposed. The mathematical details of this dynamic model will be given in the following sub-section.*

Given the initial and boundary conditions listed above, the convection and diffusion equation (2.3) can be solved numerically. The computer code developed for this purpose was based on a two-stage corrected Euler formulation with a central difference approximation in y direction and an upwind scheme in x direction, which is similar to that used in (John & Barakat [2001]).

Although the shear stress induced cellular response of VECs has been an active research subject since late 1980s (Ando *et al.* [1988]), the precise mechanism of shear stress-induced ATP release still remains elusive. Possible mechanisms include exocytosis of secretory vesicles that contain ATP (Bodin & Burnstock [2001a]), ATP release via ATP channels or transporters (Grygorczyk & Hanrahan [1997]; Sprague *et al.* [1998]), or ATP generation on the cell surface (Yamamoto *et al.* [2007]). In consideration of all these possibilities mentioned above, the following assumptions are in order.

Assumption 1. *The ATP release rate depends upon the magnitude of the wall shear stress.*

Assumption 2. *The ATP release rate is dependent on the quantity of exocytosis of secretory vesicles that contain ATP, ATP channels or transporters, and ATP generation on the cell surface.*

Assumption 3. *The ATP release rate also relies on the activation levels of the various ATP release pathways mentioned in Assumption 2.*

Based upon these assumptions, the ATP release rate $S_{\mathrm{ATP}}(\tau_w, t)$ may be described by

$$S_{\mathrm{ATP}}(\tau_w, t) = p_1 p_2, \tag{2.10}$$

where the state variable, p_1, summarizes both the effects of wall shear stress and the probability of the open states of all possible ATP release pathways, and the state variable, p_2, describes the activation levels of the various ATP release pathways mentioned in Assumption 2, which satisfy the following equations

$$\frac{dp_1}{dt} = f(\tau_w) - \frac{p_1}{\tau_1}, \tag{2.11}$$

and

$$\frac{dp_2}{dt} = -\frac{p_2}{\tau_2}, \tag{2.12}$$

where τ_1 and τ_2 represent the time delay constants; $f(\tau_w)$ is a function of the shear stress, τ_w. By carefully analyzing Yamamoto's experimental data (Yamamoto *et al.* [2003]), $f(\tau_w)$ is proposed to take the following form,

$$f(\tau_w) = a_1 + \frac{a_2 \tau_w}{a_3 + \tau_w}, \tag{2.13}$$

where a_1, a_2, a_3 are constant parameters to be determined by experimental data.

Remark 2. *It is worth noting that $f(\tau_w)$ bears the same form as that of the well known Hill function, widely used in modeling cell functions in biochemistry, which captures the common characteristic of many cellular responses to stimuli that the intensity of the response would increase with the intensity of the stimulus, but with a saturation point. The offset term, a_1, which is usually very small as shown later, is included to take into account of possible natural ATP release; for instance, VECs always weakly release ATP.*

Remark 3. *The purpose of including the state variable p_2 in the dynamic model* (2.10) *is to capture the characteristic of "receptor desensitization" (Uchida [1996]), the well known phenomenon in many cellular responses to constant stimulus, which implies that*

all the "mechano-receptors" in VECs will be passivated after being activated for a while by a constant stimulus. Despite the fact that currently there is no direct experimental evidence to establish such a phenomenon in the shear stress induced ATP release process, we speculate that "receptor desensitization" also occurs in this event since it is such a common phenomenon in many cellular responses of biological systems.

At time $t = 0$, the ATP release rate $S_{\mathrm{ATP}}(\tau_w, t)$ is taken to be zero, and the phenomenon of "receptor desensitization" does not occur, therefore, the initial conditions are expressed as follows

$$p_1(0) = 0, \tag{2.14}$$

and

$$p_2(0) = 1. \tag{2.15}$$

The equations (2.10)-(2.15) describe the dynamic model of the ATP release rate, where a_1, a_2, a_3, τ_1 and τ_2 are the ATP release constants, i.e., the model parameters, to be determined by experimental data.

Yamamoto and her co-workers (Yamamoto *et al.* [2003]) published their experimental data about the average net ATP release rate $S_{\mathrm{net,ATP}}$ against time t using human pulmonary artery endothelial cells exposed to a stepwise increasing fluid shear stress ($0 \rightarrow 0.3 \rightarrow 0.8 \rightarrow 1.5$Pa). In this case, we can easily obtain the analytical solution of Eqs.(2.10)-(2.15) as follows

$$p_1(t) = \begin{cases} \tau_1 f(\tau_{w_1}) \left(1 - e^{-t/\tau_1}\right), t \in [0, T_1] \\ \tau_1 e^{-t/\tau_1} \left[f(\tau_{w_1}) \left(e^{T_1/\tau_1} - 1\right) + f(\tau_{w_2}) \left(e^{t/\tau_1} - e^{T_1/\tau_1}\right)\right] \\ t \in [T_1, T_2], \\ \tau_1 e^{-t/\tau_1} \left[f(\tau_{w_1}) \left(e^{T_1/\tau_1} - 1\right) + f(\tau_{w_2}) \left(e^{T_2/\tau_1} - e^{T_1/\tau_1}\right)\right. \\ \left. + f(\tau_{w_3}) \left(e^{t/\tau_1} - e^{T_2/\tau_1}\right)\right], t \in [T_2, T_3] \end{cases} \tag{2.16}$$

and

$$p_2(t) = e^{-t/\tau_2}, \tag{2.17}$$

where $\tau_{w_1} = 0.3, \tau_{w_2} = 0.8, \tau_{w_3} = 1.5, T_1 = 60, T_2 = 120$ and $T_3 = 180$.

The model parameters will be computed by minimizing the difference, E, between experimental and corresponding model-predicted net ATP release rate, defined as

$$E(a_1, a_2, a_3, \tau_1, \tau_2) = \sum_{n=1}^{N} \left(S_{\mathrm{net,ATP}_{\mathrm{predicted}}}(n) - S_{\mathrm{net,ATP}_{\mathrm{exp}}}(n)\right)^2, \tag{2.18}$$

Table 1: Parameters for Original and Modified Dynamic ATP Release Model

Parameter	Unit	Value	Source
L	M	0.025	
h	μm	200	Yamamoto *et al.* [2000b]
μ	Nsm^{-2}	9.45×10^{-4}	
D	$\mathrm{m}^2\mathrm{s}^{-1}$	2.36×10^{-10}	
K_m	μM	475	John & Barakat [2001]
$V_{\max}$	$\mathrm{molm}^{-2}\mathrm{s}^{-1}$	0.8×10^{-6}	
a_1	$\mathrm{molm}^{-2}\mathrm{s}^{-2}$	0.65×10^{-13}	
a_2	$\mathrm{molm}^{-2}\mathrm{s}^{-2}$	2.79×10^{-10}	
a_3	Pa	6.96	Original dynamic model
τ_1	s	17.4	
τ_2	s	218.9	
a_1	$\mathrm{molm}^{-2}\mathrm{s}^{-2}$	4.9×10^{-13}	
a_2	$\mathrm{molm}^{-2}\mathrm{s}^{-2}$	6.7×10^{-11}	Original dynamic model
a_3	Pa	1.06	without p_2
τ_1	s	10.1	
$\bar{a}_2$	$\mathrm{molm}^{-2}\mathrm{s}^{-2}$	0.36×10^{-10}	
$\bar{a}_3$	Pa	0.53	
$\bar{\tau}_1$	s	16.32	Modified dynamic
$\bar{\tau}_2$	s	300	model
λ	Pa^{-1}	3	
S_{max}	$\mathrm{molm}^{-2}\mathrm{s}^{-1}$	3×10^{-10}	John & Barakat [2001]

where N is the total number of experimental samples, $S_{\mathrm{net,ATP_{exp}}}(n)$ is the observed value of the n-th experimental sample point. The model-predicted net ATP release rate, $S_{\mathrm{net,ATP_{predicted}}}(n)$ is expressed as

$$S_{\mathrm{net,ATP_{predicted}}} = S_{\mathrm{ATP}}(\tau_w, t) - \frac{1}{L}\int_0^L \frac{V_{\max} c \mid_{y=0}}{K_{\mathrm{m}} + c \mid_{y=0}} dx. \tag{2.19}$$

The calculation of Eq.(2.19) should take the governing equations (2.3)-(2.5) and their corresponding boundary and initial conditions into consideration. The average value in the direction of x is taken in Eq.(2.19) since the experimental measurements of the net ATP release rate, $S_{\mathrm{net,ATP_{exp}}}$, were obtained as averaged values in the experiments (Yamamoto *et al.* [2003]). We adopt aforementioned numerical difference scheme with Nelder-Mead simplex algorithm (Lagarias *et al.* [1998]; Nelder & Mead [1965]) to obtain the model parameters, i.e., release constants, as shown in Table 1. The other model parameters required by the numerical simulations are also listed in Table 1.

2.2.2 Simulation Results

Fig 2.2 shows the net ATP release rate against time under a stepwise increasing fluid shear stress ($0 \rightarrow 0.3 \rightarrow 0.8 \rightarrow 1.5$Pa). The dots correspond to Yamamoto's experimental results (Yamamoto *et al.* [2003]). The solid line is the result fitted by our dynamic model of the ATP release rate, given in equations (2.3)-(2.15), and the dashed line is the result fitted by John and Barakat's linear static model as shown in Eq (2.1). For purpose of comparison, we also considered the possibility that the phenomenon of "receptor desensitization" may not occur (assuming $p_2 = 1$ in Eq (2.17)), and fitted the experimental data about the net ATP release rate against time as shown in Fig 2.2 The release constants were obtained, as listed in Table 1. The fitting result is plotted out as dash-dotted line in Fig 2.2. The data fitting was conducted in Matlab with the command "fmincon" to determine all the parameters. Before the optimization, a biologically reasonable range was assigned to each parameter. The total time to obtain the final parameters was about one hour with a Fujitsu S6210 laptop.

It is interesting to note that the fitting result by the dynamic model without p_2 (dash-dotted line) is also very close to experimental observations, which motivates us to initiate further investigation on whether taking into consideration the phenomenon of "receptor desensitization", i.e. including p_2 in the model, is really crucial or not. In order to address this issue, we design the following simulated experiment to make the

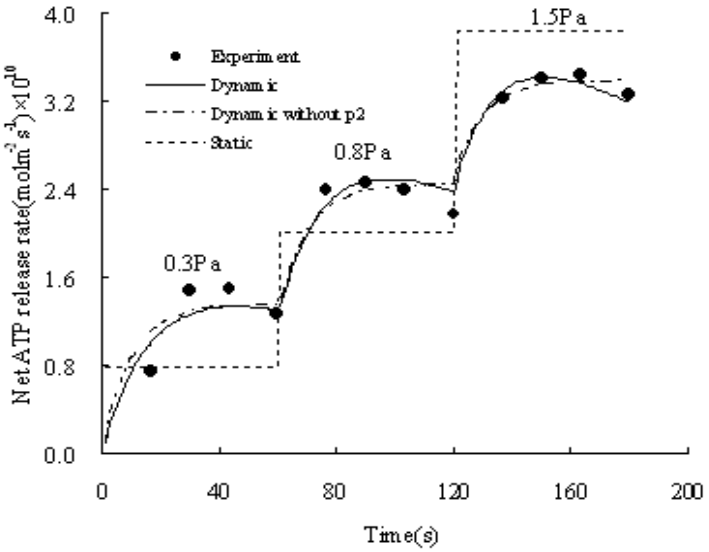

Figure 2.2: Comparison between experimental and corresponding model-predicted average net ATP release rate S_{ATP} against time t from the onset of steady fluid shear stress in a stepwise manner ($0 \rightarrow 0.3 \rightarrow 0.8 \rightarrow 1.5$Pa)

predictions of the models with/without p_2 significantly different, and compare them to the existing experimental results available in the literature.

Fig 2.3 demonstrates the predicted dynamic behaviors of the average value of extracellular ATP concentration in the endothelial cell surface from the onset of steady fluid shear stress in a stepwise manner ($0 \rightarrow 0.4 \rightarrow 1$Pa). The solid lines correspond to the predicted extracellular average ATP concentration against time by dynamic model; the dashed lines show the predicted extracellular average ATP concentration against time by John and Barakat's linear static model; and the dash-dotted lines correspond to the predictions made by the model without p_2. We intentionally make the time duration of the second steady flow very large (800 seconds) such that the effect of the "receptor desensitization" (if exists) might be substantial which hopefully would lead to large difference between the predictions of the various models.

It can be readily seen from Fig 2.3 that the average ATP concentration at endothelial surface in steady flow predicted by our dynamic model is indeed dramatically different from those predicted by the static model and the dynamic model without p_2. In particular, after ECs being activated for a long time by a step shear stress 1Pa, while both the static model and dynamic model without p_2 predict steady stable concentration, the dynamic model predicts a gradually decreasing response. Which one is more

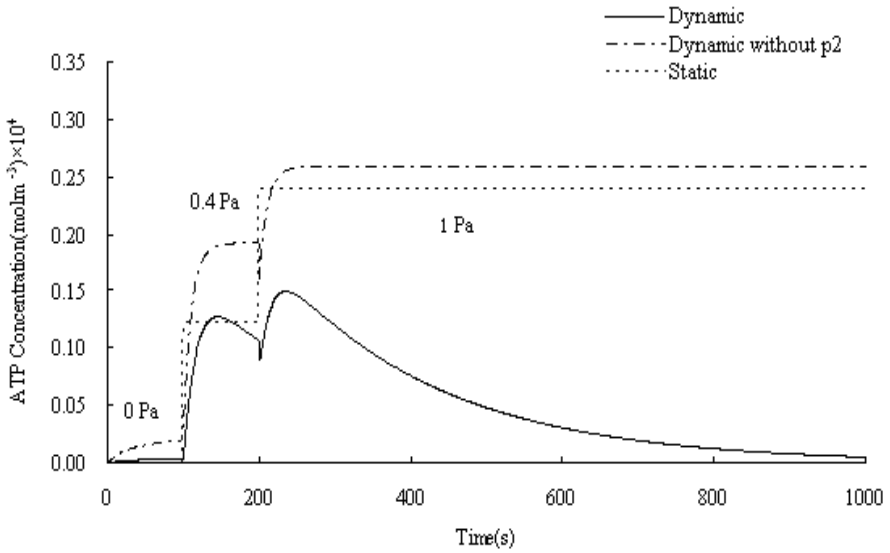

Figure 2.3: Comparison between dynamic and static model-predicted extracellular ATP concentration in the endothelial cell surface against time from the onset of steady fluid shear stress in a stepwise manner ($0 \rightarrow 0.4 \rightarrow 1$Pa)

accurate? There are some indirect experimental evidences, such as the experiment carried out on human umbilical vein endothelial cells (HUVECs) by Bodin and Burnstock (Bodin & Burnstock [2001a]). It is clearly manifested in the Fig 1 of the paper (Bodin & Burnstock [2001a]), that being activated by a small step shear stress for one period and then a larger step shear stress for a much longer period, the ATP concentration initially increases to a maximum level and then gradually decreases, which agrees qualitatively with the predictions made by our dynamic model. It is noted that the time scale of the experimental data plotted in Fig 1 by Bodin and Burnstock is much larger than the ones predicted by our dynamic model, which is due to the fact that Bodin and Burnstock used a cone-plate device. They cultured HUVECs in a petri dish and when shear stress was applied, the buffer medium would not be flushed out. Released ATP in the medium could again trigger more ATP release from HUVECs.

It is noticed that there exists a huge dip in Fig 2.3 when the shear stress increases suddenly from 0.4Pa to 1Pa. This is because the sudden change in flow velocity $v(y)$ of ATP-free perfusate will lead to the sudden increase in the convection term in Eq.(2.3), which in turn results in the abrupt decrease in the extracellular ATP concentration at the bottom of the flow chamber.

Remark 4. *It is interesting to note that after a large step shear stress being applied to*

the VECs for a sufficiently long time, the ATP concentration eventually decreases to a level which is even lower than the ones corresponding to the smaller step shear stress, as observed in Bodin and Burnstock's experiment and also predicted by our dynamical model. It is impossible for any kind of static model to account for this type of dynamic behavior, which implies that the approach of dynamic modeling is crucial.

Despite the fact that none of the real experiments related to shear stress induced ATP release on VECs have been conducted for pulsatile flow, further numerical comparison studies are carried out for predicting extracellular average ATP concentration in the endothelial cell surface under the condition of pulsatile flow, as this is more physiologically relevant to human VECs.

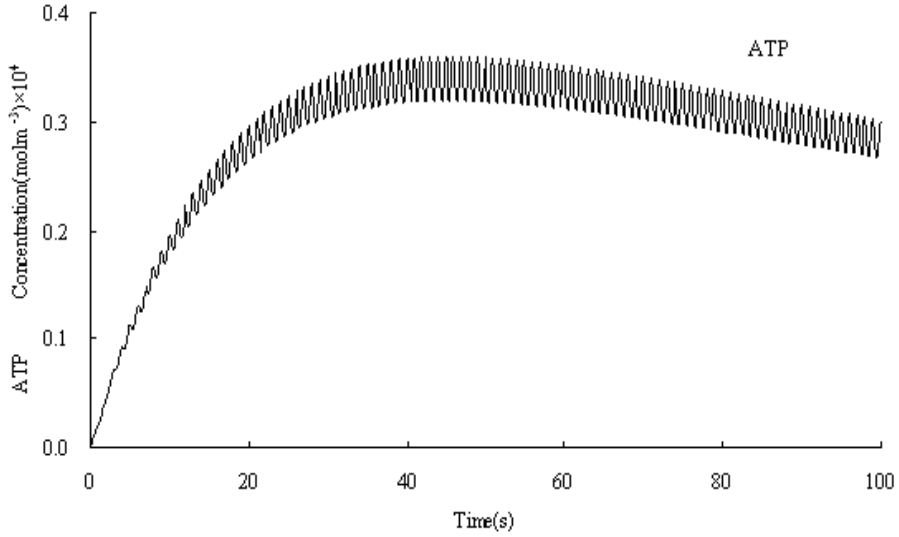

Figure 2.4: Dynamic model-predicted extracellular ATP concentration in the endothelial cell surface against time from the onset of pulsatile fluid shear stress $\tau_w = 1 + \sin(2\pi t)$, time course $0 - 100$s.

Fig 2.4 displays the dynamic behavior of the extracellular average ATP concentration in the endothelial cell surface from the onset of pulsatile fluid shear stress, $\tau_w = 1 + \sin(2\pi t)$. Fig 2.4 shows the predicted extracellular average ATP concentration against time by dynamic model. Fig 2.5 shows the predicted extracellular average ATP concentration against time by John and Barakat's linear static model. It can be readily seen from Fig 2.4 and 2.5 that while the dynamic model predicts that the average ATP concentration at the endothelial cell surface is nonstationary until about 40 seconds (see Fig 2.4), the static model predicts that the stationary state of average ATP

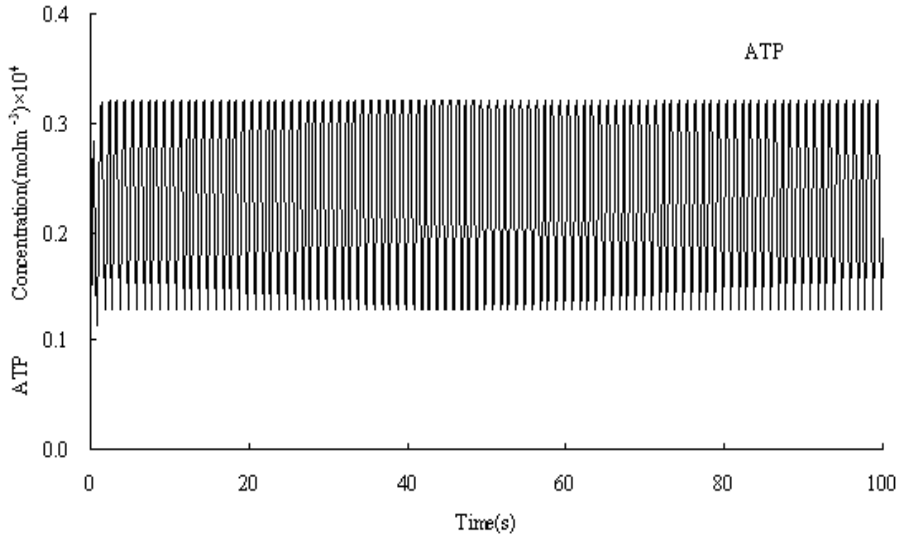

Figure 2.5: Static model-predicted extracellular ATP concentration in the endothelial cell surface against time from the onset of pulsatile fluid shear stress $\tau_w = 1 + \sin(2\pi t)$, time course $0 - 100$s.

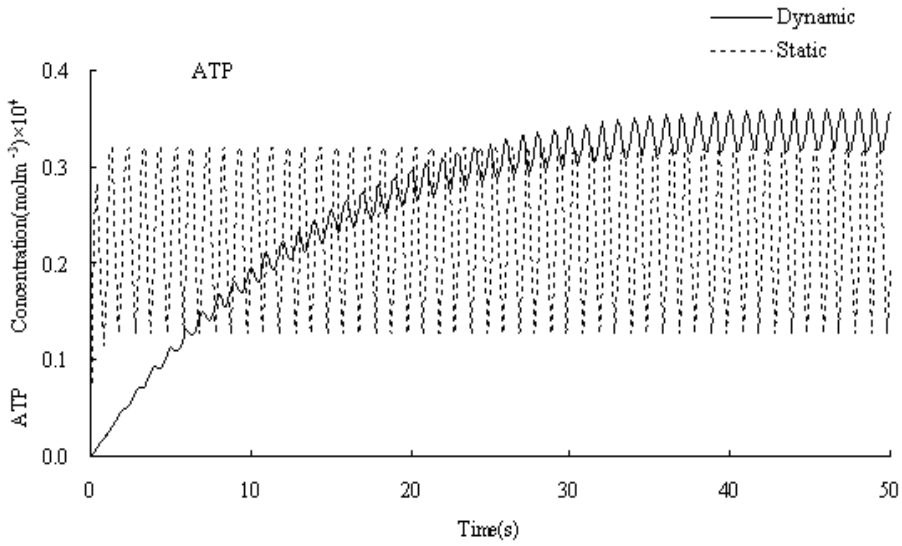

Figure 2.6: Comparison between dynamic and static model-predicted extracellular ATP concentration in the endothelial cell surface against time from the onset of pulsatile fluid shear stress $\tau_w = 1 + \sin(2\pi t)$, time course $0 - 50$s.

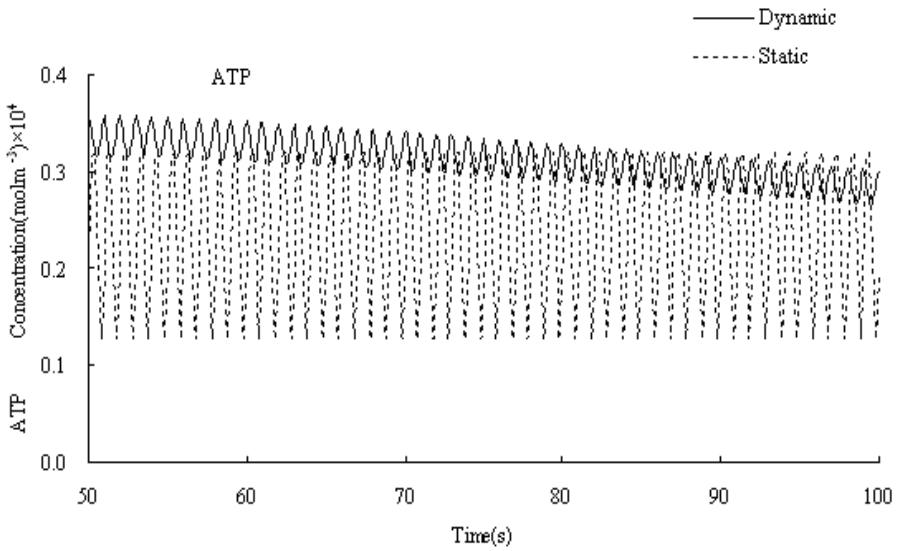

Figure 2.7: Comparison between dynamic and static model-predicted extracellular ATP concentration in the endothelial cell surface against time from the onset of pulsatile fluid shear stress $\tau_w = 1 + \sin(2\pi t)$, time course $50 - 100$s.

concentration at the endothelial cell surface is attained within a few seconds (see Fig 2.5). It is noticed from Fig 2.4 - 2.7 that, during the initial period right after the onset of pulsatile flow, the dynamic behavior of the average ATP concentration at endothelial surface predicted by our dynamic model is quite different from that predicted by the static model. However, after around 40 seconds, both the dynamic and static models predict very similar characteristic of the ATP concentration at endothelial surface: an oscillation with the same period of 1 second as that of the pulsatile flow.

It is interesting to note that the predicted amplitudes of the oscillations are also quite different. In the static model, as the amplitude of the ATP release rate is directly related to the amplitude of the shear stress, which is assumed to be a constant, it naturally predicts an oscillation with constant amplitude. However, in the dynamic model, the amplitude of the ATP release rate depends upon both the amplitude of the shear stress and the time in a dynamic fashion. Hence it is observed in Fig 2.4 - 2.7 that the amplitude predicted from the dynamic model is not only smaller, but also slowly varying with time.

It is difficult to validate the predictions of the dynamic model and static model due to lack of experimental observations in the literature under the condition of pulsatile flow. It remains to be verified later by future experiments for pulsatile flows.

Remark 5. *It is also noticed that the magnitude of the ATP concentration predicted by the dynamic model gradually decreases with time in the long run, due to effect of "receptor desensitization" factor p_2. However, it is well known that "receptor desensitization" usually happens only when the stimulus is a constant. When the stimulus is a time-varying signal, there could be other activation mechanism to balance this desensitization.*

2.3 Modified Dynamic ATP Release Model

In the previous section, a dynamic model is suggested to describe the time-dependency of shear stress induced ATP release rate, which leads to better data fitting as well as predictions more consistent with experimental evidence (Yamamoto *et al.* [2003]). However, the predicted ATP concentration under time-varying stimulus seems unreasonable due to lack of activation mechanism.

In this section, we aim to develop a modified dynamic model to incorporate the activation mechanism caused by time-varying shear stress on the basis of the original dynamic model. Different predictions of ATP concentration on VECs surface are demonstrated through simulation studies. The governing equation depicting the convection and diffusion process of ATP remains valid. The major modification is made on the ATP release rate $S_{ATP}(\tau_w, t)$, where the changing rate of shear stress is considered to be the activation mechanism.

2.3.1 Activation Mechanism: via Time-varying Shear Stress

We keep the structure of the ATP release rate term developed in previous section as

$$\bar{S}_{ATP} = \bar{p_1}\bar{p_2}, \tag{2.20}$$

where the state variable $\bar{p}_1$, summarizes both the effects of wall shear stress and the open states of all possible ATP release pathways. The state variable $\bar{p}_2$ describes the probability that various ATP release pathways are all open. Therefore, $\bar{p}_2$ has a lower bound of 0 and upper bound of 1. Note that we employ the bar notation in the modified model to avoid confusion with the original one. They satisfy the following equations

$$\frac{d\bar{p}_1}{dt} = \bar{f}(\tau_w) - \frac{\bar{p}_1}{\bar{\tau}_1}, \tag{2.21}$$

and

$$\frac{d\bar{p}_2}{dt} = -\frac{\bar{p}_2}{\bar{\tau}_2} + \lambda \frac{d\tau_w}{dt}, \qquad \bar{p}_2 \in [0, 1], \tag{2.22}$$

where $\bar{\tau}_1$ and $\bar{\tau}_2$ represent the time delay constants; λ is a positive coefficient; $\bar{f}(\tau_w)$ is a function of the shear stress τ_w in the form of

$$\bar{f}(\tau_w) = \bar{a}_1 + \frac{\bar{a}_2 \tau_w}{\bar{a}_3 + \tau_w}, \tag{2.23}$$

where $\bar{a}_1, \bar{a}_2$ and $\bar{a}_3$ are positive constants. In the original dynamic model, a_1 is included to describe possible natural ATP release, which turns out to be very small. Since this term is negligible, it is assumed to be zero in the modified model for simplicity purpose.

In the original dynamic model, the state variable p_2 is intended to capture the characteristic of "receptor desensitization". Since p_2 is independent of shear stress in that model, it is always decreasing with time, which implies that the ATP release will decrease in the long run. However, it is well known that "receptor desensitization" usually happens only when the stimulus is a constant. When the stimulus is a time-varying signal, there could be other activation mechanism to balance this desensitization. In order to incorporate this activation mechanism, the dynamics of $\bar{p}_2$ in this modified dynamic model is proposed to depend also on the change rate of shear stress as shown in Eq (2.22).

At $t = 0$, the ATP release rate $\bar{S}_{ATP}(\tau_w, t)$ is taken to be zero and initial conditions are expressed as follows

$$\bar{p}_1(0) = 0, \tag{2.24}$$

and

$$\bar{p}_2(0) = 0. \tag{2.25}$$

All the parameters, i.e., $\bar{a}_2, \bar{a}_3, \bar{\tau}_1, \bar{\tau}_2$ and λ, are to be determined by experimental data Yamamoto *et al.* [2003], which can be handled in the same manner described in the previous section.

2.3.2 Simulation Results

Fig 2.8 shows the net ATP release rate against time under a stepwise increased shear stress. It is evident from Fig 2.8 that while the results fitted by linear static model show poor agreement with experimental data, the results fitted by our two dynamic models exhibit satisfactory agreements with the experimental results (Yamamoto *et al.* [2003]).

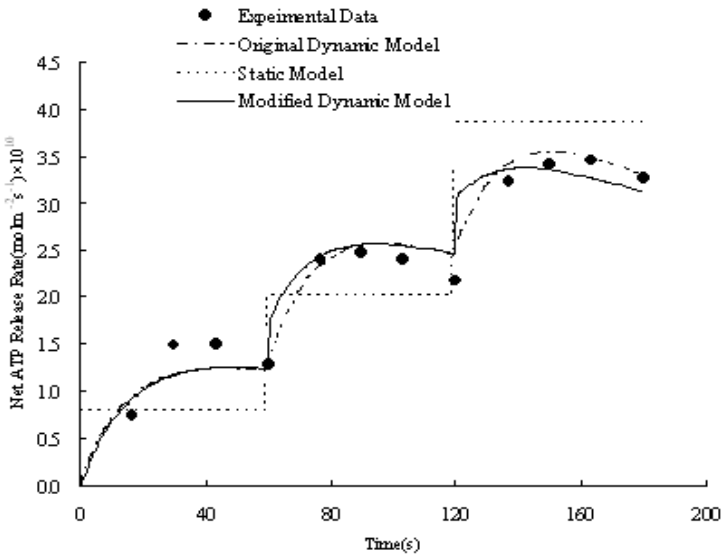

Figure 2.8: Comparison between experimental and corresponding model-predicted average net ATP release rate $S_{net,ATP}$ against time t from the onset of steady fluid shear stress in a stepwise manner ($0 \rightarrow 0.3 \rightarrow 0.8 \rightarrow 1.5$Pa).

There is a sharp jump in the modified dynamic model-predicted ATP release rate during the periods when the shear stress suddenly increases from 0.3 to 0.8Pa and from 0.8 to 1.5Pa while the net ATP release rate curve fitted by the previous dynamic model is quite smooth. Such a difference is caused by the activation mechanism incorporated in the modified dynamic model since a sudden increase in shear stress will lead to a jump in $\bar{p}_2$ and hence in the net release rate of ATP. However, it is still difficult to tell which of the two dynamic models gives a more accurate picture of net ATP release rate as the experimental data are sampled every 15 seconds in (Yamamoto *et al.* [2003]).

Fig 2.9 demonstrates the predicted dynamic behaviors of the average extracellular ATP concentration at VECs surface under stepwise manner shear stress stimulation. All the model parameters required by numerical simulations are listed in Table 1.

It can be readily seen from Fig 2.9 that the average ATP concentrations predicted by our two dynamic models are indeed dramatically different from that predicted by the static model. In particular, after VECs being activated for a long time. The static model predicts a stable concentration while the dynamic models predict a gradually decreasing response. Unfortunately there is no direct experimental evidence existing in the literature for us to make judgment on which one is more reasonable.

We intentionally make the shear stress decrease from 0.5 to 0.4Pa at 300 second

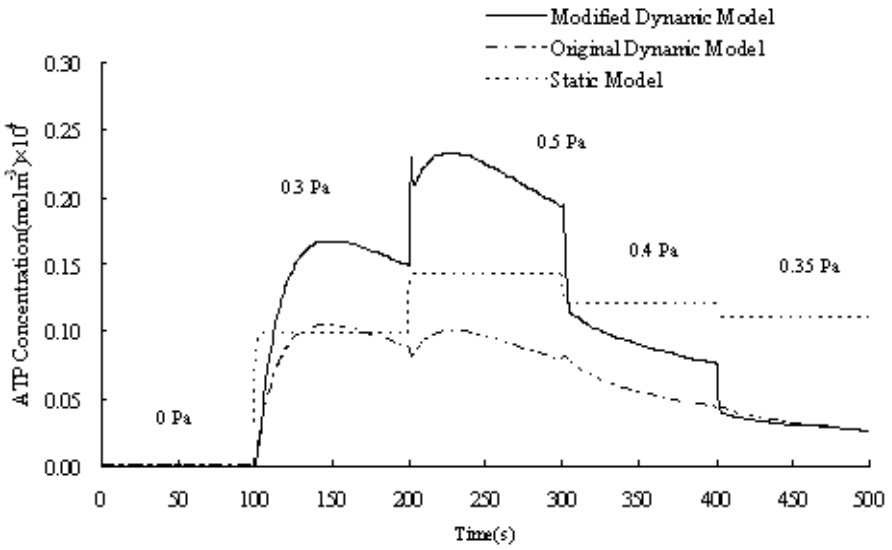

Figure 2.9: Comparison between dynamic and static model-predicted extracellular ATP concentration in the endothelial cell surface against time from the onset of steady fluid shear stress in a stepwise manner ($0 \rightarrow 0.3 \rightarrow 0.5 \rightarrow 0.4 \rightarrow 0.35$Pa).

and then to 0.35Pa at 400 second in order to see different behaviors of ATP concentration predicted by the modified and original dynamic models. The ATP concentration predicted by the original dynamic model does not have an obvious response to the decreased shear stress. However, in the modified dynamic model, there is a sudden drop of ATP concentration corresponding to the sudden decrease of shear stress. Direct experimental evidence is needed to help us judge which of the two predictions is closer to the real case.

Fig 2.10 and 2.11 display the dynamic behaviors of the extracellular average ATP concentration at VECs surface from the onset of pulsatile fluid shear stress.

It is noticed from Fig 2.10 that, during the initial period right after the onset of pulsatile flow, the dynamic behaviors of the average ATP concentration at endothelial surface predicted by our dynamic models are quite different from that predicted by the static model. However, after around 40 seconds, both the two dynamic models and static model predict a very similar characteristic of the ATP concentration at endothelial surface: an oscillation with the same period of 1 second as that of the pulsatile flow, even though the predicted magnitudes of oscillations are quite different.

It is also noticed that the magnitude of the oscillation predicted by the original dynamic model gradually decreases with time in the long run, due to the effect of "receptor desensitization", which usually occurs to a constant stimulus. Therefore the modified

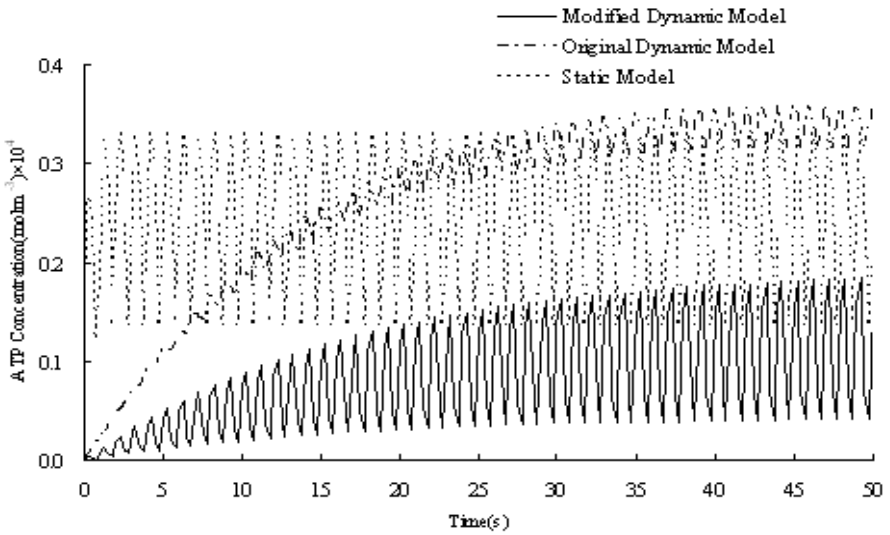

Figure 2.10: Comparison between dynamic and static model-predicted extracellular ATP concentration in the endothelial cell surface against time from the onset of pulsatile fluid shear stress $\tau_w = 1 + \sin(2\pi t)$, time course $0 - 50$s.

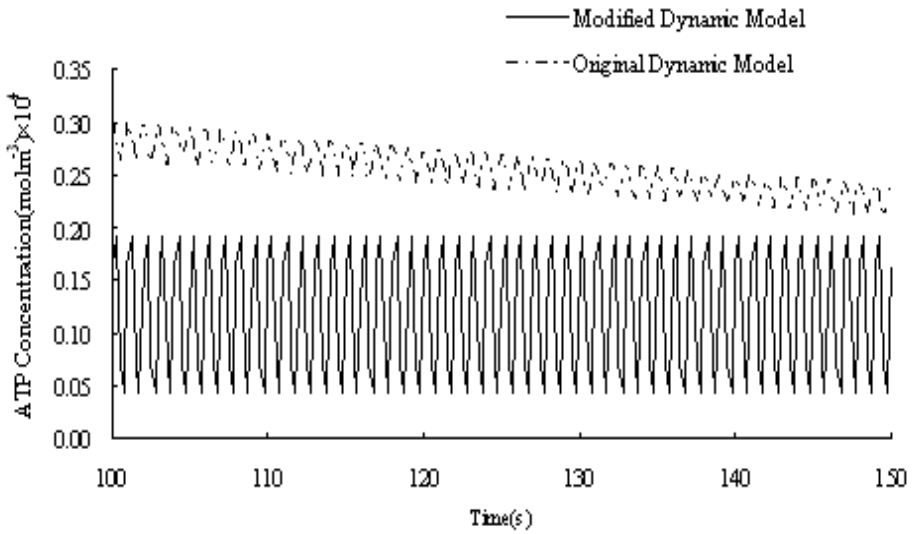

Figure 2.11: Comparison between dynamic and static model-predicted extracellular ATP concentration in the endothelial cell surface against time from the onset of pulsatile fluid shear stress $\tau_w = 1 + \sin(2\pi t)$, time course $100 - 150$s.

dynamic model-predicted ATP concentration seems to be more reasonable in face of a time-varying sinusoidal shear stress. As can be seen from Fig 2.10, the magnitude of its oscillation tends to stay within a fixed range. We omit the dynamic behaviors of ATP concentration for the static model in order for a clearer demonstration. It is not hard to imagine that during this period, the ATP concentration predicted by the static model tend to oscillate in the same manner as shown in Fig 2.11.

It is difficult to validate the predictions of the two dynamic models and the static one due to lack of experimental observations in the literature under the condition of pulsatile flow. It remains to be verified later by future experiments for pulsatile flow.

2.4 Dynamic Model of ATP Release: with Limited Reactivation Capacity

As discussed in previous two sections, the advantage of dynamic model becomes quite obvious. The original dynamic model can foresee a declining trend of ATP release when cells are exposed to constant shear stress for a long time. The modified dynamic model include further the reactivation mechanism, by which the capacity of ATP release in VECs could be restored as long as there is a change in shear stress.

However, these two models are a little bit too "ideal". A batch of cells, with living features is very different from machines. Cells could only sense and undertake the stimulus in a physiologically reasonable range. And they have limited capacity to make responses. Like we human beings, a good rest is essential for daily work.

The drawback of original dynamic model lies in the lack of reactivation mechanism while the modified one overemphasizes cells capacity of ATP release. Even being stimulated by time-varying shear stress for hours, cells could give very positive response, which seems quite contradict to our common physiological understanding. That is why we propose a third dynamic model in which cells could be reactivated under certain conditions. For simplicity, we name it SAT dynamic ATP release model. SAT is the abbreviation of saturation.

2.4.1 Activation Mechanism: Limited Capacity of Reactivation

Before we formulate the mathematical expression of SAT dynamic ATP release model, two assumptions limiting excessive reactivation are posed as follows,

Assumption 4. *The reactivation level is time-dependent when VECs are continuously exposed to shear stress. The reactivation capacity is weakened as stimulation time goes*

by.

Assumption 5. *VECs could only sense shear stress change in a physiologically reasonable range. A too large change will be filtered while a too small one be neglected.*

Based on the above two assumptions, we modify the p_2 term to be

$$\frac{d\tilde{p}_2}{dt} = -\frac{\tilde{p}_2}{\tilde{\tau}_2}\left[1 - \tilde{\lambda}\exp(-t/\tilde{\tau}_3)sat(\dot{\tau}_w, t)\right], \tag{2.26}$$

where $sat(\dot{\tau}_w, t)$ is expressed as

$$sat(\dot{\tau}_w, t) = \begin{cases} -1 & \dot{\tau}_w \leq -\dot{\tau}_0 \\ \dot{\tau}_w/\dot{\tau}_0 & -\dot{\tau}_0 < \dot{\tau}_w < \dot{\tau}_w \\ 1 & \dot{\tau}_w \geq \dot{\tau}_0 \end{cases} \tag{2.27}$$

and $\tilde{\lambda} > 1$.

It is noted that $\tilde{\tau}_2, \tilde{\tau}_3$ are time constants and $\dot{\tau}_0$ is the upper bound of shear stress change that could be sensed by VECs. These parameters are to be determined by data fitting as described previously.

Here we omit the tedious simulation results as they are supposed to be easily obtained following the computational schemes in original and modified dynamic models. The modification is minor in terms of mathematical structure but is significant viewed from a physiological perspective.

2.5 Discussion

Although a number of investigations by *in vitro* cell experiments have established that shear flow induces ATP release from endothelial cells (Bodin & Burnstock [2001a]; Guyot & Hanrahan [2002]), few quantitative analysis of the relationship between the shear stress and ATP release rate has ever been reported in the literature. The static model first proposed by John and Barakat (John & Barakat [2001]) captured a number of essential features of the shear-stress-induced ATP release process, a questionable assumption was made in their static models, that is, once a step shear stress acts on VECs, they immediately release ATP, with release rate being a constant, which is independent of the time, which apparently does not agree with the experimental evidences very well (Bodin & Burnstock [2001a]; Guyot & Hanrahan [2002]; Yamamoto *et al.*

[2003]). As shown in Fig 2.2, the result fitted by the static model shows unsatisfactory agreement with experimental results.

It is for the purpose of considering the time-dependency of the ATP release rate that a dynamic model is proposed and simulated in this chapter. It can be readily seen from Fig 2.3 and that the theoretical results (solid lines) fitted by our dynamic models exhibit adequate agreement with the experimental results by Yamamoto and her colleagues (Yamamoto *et al.* [2003]), which implies that our time-dependent models, at least from phenomenological point of view, are reasonable.

It is speculated that "receptor desensitization" occurs in the process of shear-stress-induced ATP release, i.e., all the ATP release pathways would be closed after being activated for a long time by a step shear stress, which essentially implies that it is the variation of the shear stress that induces the ATP release. Although at present there is no direct experimental evidence to support or refute this speculation, we are encouraged by the experimental work of Bodin and Burnstock (Bodin & Burnstock [2001a]), which shows that the ATP concentration would gradually decrease to a very small level when a constant shear stress acts on the VECs for a long time.

Based upon the dynamic model for shear-stress-induced ATP release, the ATP concentration at the outer surface of ECs cultured in the bottom of parallel-plate flow chamber in pulsatile flow has been studied by numerical simulations. It is demonstrated that the dynamic behavior of the ATP concentration at endothelial surface in pulsatile flow predicted by our dynamic model is quite different from that predicted by static model. In the initial stage after the onset of flow, the static model predicts that the steady state of ATP concentration at the endothelial cell surface is attained within a few seconds, but the dynamic model predicts that peak ATP concentration at the endothelial cell surface is achieved around 40 seconds. The difference may affect the intracellular calcium dynamic in VECs. The static model would predict much faster calcium response than the dynamic model does. However, the dynamical behavior predicted by the dynamic model appears more reasonable because the intracellular calcium response in VECs usually occurs in 15-40s after steady shear stress is applied on VECs.

In following chapter, we are to design and fabricate the device with which shear-stress-induced ATP release could be measured. And performance of the three models could be clearly ranked.

Chapter 3

Design and Fabrication of Perfusion/Flow System for Shear-stress-induced ATP Measurement

We have investigated the distribution of released ATP from VECs when different flow patterns (and thus different shear stresses) are applied on cell surface in Chapter 2. Based on experimental data available in literature, we have built three dynamic shear-stress-induced ATP release models, which bear distinct receptor desensitization and reactivation mechanisms, respectively.

In this chapter, we first introduce the design and fabrication of a chamber like device, named "perfusion/flow system", with which various kinds of shear stress could be applied and released ATP would be measured. The performance of the three established models would be easily ranked with our own experimental results.

Compared to the commercial flow chamber, the perfusion/flow system integrates cell culture and flow loading test into one single bio-chip. Our observations have (1) shown that VECs can grow properly in perfusion/flow system and (2) verified that receptor desensitization exists in VECs and the capacity for reactivation is limited.

3.1 Integrate Cell Experiments in A Single Chip

Lab on a chip refers to the integration of some experimental routine occurred in lab into one single chip. This concept and its application in analytical devices could be

traced back in the 1990s (Manz *et al.* [1992]). The past two decades have witnessed a big boost in the development of technologies that contribute to lab-on-chip (McDonald *et al.* [2000]; Whitesides [2006]). Due to the small size of the chip (usually around 100 microns or even smaller), it is an ideal choice for mimicking some micro-environment in living body. Furthermore, the consumption of the reagents will be dramatically reduced as the chip is highly compact in terms of its size and functions as well. That is why such delicate and economical device has been so popular these years. Generally speaking, a successful cellular experiment based on biochips requires:

1. A good design of the chip to meet a specific experimental requirement.
2. Matured technology and proper materials for fabrication.
3. Deep understanding of the interaction between the cell behaviors and the chip environment from both biological/physiological and engineering perspectives.
4. Proficient skills in handling cells and chip.

In our case, we need to integrate cell culture, ATP release measurement and Ca^{2+} imaging into the one system. The main reason for doing so is that it is more economical and total experiment span is reduced as cell would grow faster in the environment with continuous nutrient perfusion.

3.2 Design and Fabrication of Perfusion/Flow System

As indicated by its name, "perfusion/flow system", the device has two main functions. Nutrients would be perfused at a very slow rate to the cells growing in the chamber. When cells are ready for experiments, different flow patterns could be applied to mimic the real situation in human blood vessels. The detailed design considerations and fabrication procedures are discussed in the following subsection.

3.2.1 Some Considerations in System Design

We choose the glass slide as the substrate for culturing cells and polydimethylsiloxane (PDMS) be the chamber cover on which the design pattern is etched. Attached mammalian cells could grow well on glass slide. PDMS is a popular material used by many researchers as substrate as it is not toxic to cells and with good gas permeability.

Fig 3.1 shows the patterns for ATP release measurement (bottom) and calcium imaging (top), respectively. The main difference of the two patterns lies in the number

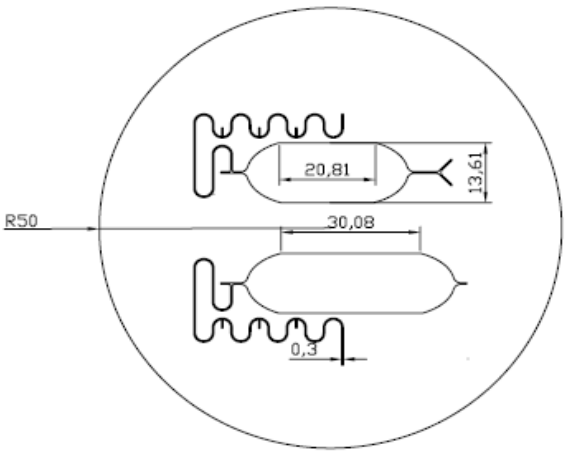

Figure 3.1: Draft of pattern etched on PDMS cover. The top one is used for calcium imaging test. It has two inlets, one for buffer medium containing ATP and the other for medium free of ATP. Streams from the two inlets would mix together and generate time-varying input signals. The bottom one only has one inlet and is designed for measuring ATP release under different shear stresses. The winded channels are kept open till cells are ready for experiments. They would largely increase the chamber resistance so that nutrient would perfuse at a slow rate. During flow loading test, these winded channels are blocked and the exit is opened, switching the whole system to its flow mode. Unit: mm

of inlets. For ATP measurement, we have only one inlet and one outlet because flow (containing no APT) alone is sufficient to trigger ATP release. However, for calcium imaging, we have to regulate the shear stress and ATP level as well so as to obtain a desirable response. That's the reason why we need to mixing two streams of flow – one with high level of ATP and the other free of ATP to generate time-varying shear stress and ATP signals. The utilization of such time-varying signal (dynamic ATP and shear stress) would guarantee a long lasting calcium response, as will be discussed in detail in Chapter 5. The twisted and narrow channels are designed for increasing system resistance. We block the outlet and leaves these channels open until cells are ready for experiments. During the growth process, continuous nutrients could be perfused to the system at a rather slow rate due to large resistance generated by the winded channels. Before the flow loading test, the outlet is reopened while these winded channels are blocked, switching the system status from perfusion to flow loading.

By modifying the diameter and length of the winded channels, we can obtain perfusion/flow system with different perfusion rates. The oval part in the center is for cell culture. Its area could also be enlarged if more cells are required for the experiments.

3.2.2 Master Fabrication via Photolithography

The first step in device fabrication is to manufacture a master (or a molder) imprinted with the design. A Silicon wafer is chosen as the substrate (Thanks to Prof. Arthur Tay's generous gifts) on which the light-sensitive emulsion SU8 is spin-coated. The thickness of the coated SU8 is about 100-150 microns according to later measurements from OCT. The wafer with a thin layer of SU8 is then baked on a hot plate for about 25 minutes at 60 degree before exposed to a selective wavelength for 120s. Post baking lasts for 30 minutes at 90 degree. At this stage, we could clearly see the image appearing on SU8. Use SU8 developer to wash off the unexposed parts and what remains is the desired pattern.

All the procedures should be conducted in a standard clean room. After the master is produced, keep it in a dry and sealed box. As the master is fragile, it should be handled with special care.

3.2.3 Assembly of Perfusion/Flow System

To make the PDMS cover, mix the PDMS with its curing agent at a ratio of 10:1. Stir them gently for about 5 minutes, degas for 25 minutes and slowly pour it onto the master. To avoid bubble generation, pour the mixture from the side of the substrate.

Bake the master with PDMS mixture for 2 hours at 60-80 degree. Peel off PDMS slowly from the silicon substrate. Try to avoid touching the side of PDMS attaching to the substrate. Cut PDMS and punch inlets and outlet on it.

Glass slides should be washed thoroughly before binding to PDMS. It is recommended to bake both PDMS cover and glass slide in 60 degree oven for 15 minutes before plasma etching.

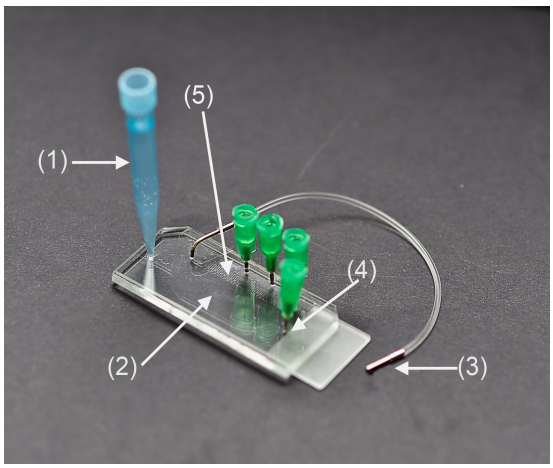

Figure 3.2: Perfusion/Flow System: (1) medium reservoir, gravity-induced flow to nurture cells; replaced by a pumping syringe to apply flow for test purpose; (2) chamber for cell growth; (3) outlet of the perfusion system, blocked during flow loading test; (4) outlet of the flow chamber, blocked during cell culture; (5) twisted channel to increase resistance for desired flow rate.

A complete set of perfusion/flow system is shown in Fig 3.2. We can see the outlet is blocked, indicating the system is set at the perfusion status. When cells are ready for experiment, take off the reservoir (the blue tip in Fig 3.2) and plug in the tube connected with a syringe pump. The resistant part should be blocked during ATP measurement and calcium imaging tests.

3.3 Dynamic Cell Culture in Perfusion/Flow System

To verify the validation of perfusion cell culture system, HUVECs are cultivated in the perfusion/flow system and the conventional T25 flask for comparison. Fig 3.3 show the growth of HUVECs at the perfusion cell culture system and T25 flask respectively. Cell statuses have been recorded right after the seeding (Fig 3.3(a)-(b)) and 20 hours (Fig 3.3(c)-(d)) after seeding. As can be seen from Fig 3.3(a) and (b), the cells are

uniformly distributed; but the image of the cells in T25 flask looks a bit more vague. This is because initially separated cells tend to float in different depths of culture medium, making it impossible to focus all cells on a single layer. On the contrary, cells in the perfusion culture system are clearly captured, indicating the separated cells are almost floating in the same level of medium. This is not difficult to understand since the main difference between the perfusion culture system and the conventional flask is the size of the space for cells to live. Given the same bottom side area, the height of the perfusion system is 0.1mm while in T25 flask, the medium is around 2-3mm.

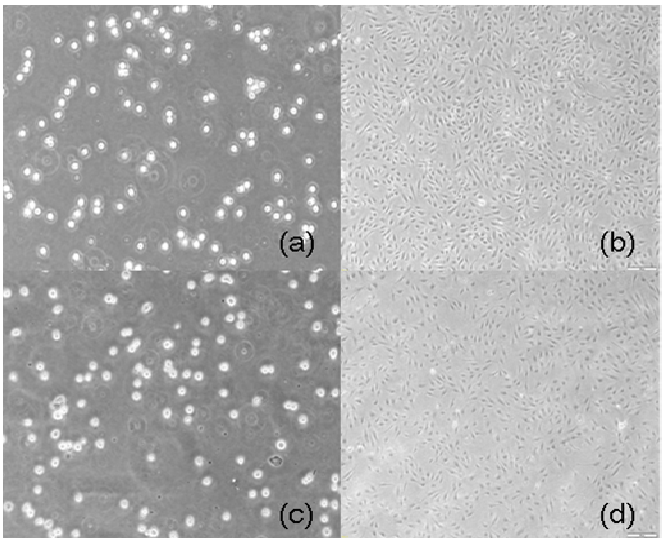

Figure 3.3: Comparison of the growth of HUVECs (passage=4) in perfusion/flow system and conventional T25 flask. Pictures (a)-(b) are taken just after HUVECs are seeded in perfusion/flow system and in T25 flask. Pictures (c)-(d) record the cell status 20 hours after seeding in perfusion/flow system and in T25 flask, respectively.

The rounded cells floating in the medium start to stretch themselves on the bottom surface and begin to show the normal morphology of HUVECs about 2 hours right after seeding. The cells in the perfusion system and T25 flask look almost the same (figures not shown here), implying the comparable cell statuses. We start the perfusion system 2 hours after seeding, introducing a very slow flow of fresh medium into the culture chamber to supply the nutrients and to wash away the waste produced by the cells. The flow rate is controlled by the medium level in the reservoir and should be properly set since a too small value will lead to inadequate gas and nutrients exchange while a too large value will cause the remodeling of endothelial cells. As to the conventional way of cell culture, there is no need to change medium in T25 flask. The medium in

the flask could sustain the cells for 24 hours.

20 hours after the seeding, cells has begun to multiply in perfusion/flow system and in T25 flask as well, as shown in Fig 3.3 (c)-(d). It can be seen in this stage, the number of cells in the perfusion/flow system exceeds that in T25 flask, implying a faster growth rate in the device with continuous medium perfusion. HUVECs in the perfusion/flow system reach confluence 20 hours after seeding and are ready for test; while in T25 flask, cells reach 80% confluence.

The micro-scaled perfusion/flow system mimics very well the real circumstances where HUVECs live; and thus facilitate the generation of shear stress whose magnitude is comparable to that existing in the veins. The observed cell statuses show the two different culture methods (i.e., in perfusion/flow system and in conventional T25 flask) are comparable. The results validate the feasibility of the cell culture in micro-scaled device, which is the foundation for the following tests.

3.4 Measurement of Shear-stress-induced ATP release

We conduct the ATP release experiment when cells are grown to 80% confluence in the perfusion/flow system. Fig 3.4 shows the results. In this 4-minute experiment, two cycles of time-various shear stress are applied directly on HUVECs surface. It can be clearly observed that ATP release amount reaches its maximum when shear stress increases to peak in the first cycle. However, this phenomenon almost disappears in the second cycle, indicating strong receptor desensitization and very limited capacity of reactivation of HUVECs. Based on this finding, we might conclude that the modified dynamic ATP release model with limited capacity of reactivation outperforms the other two, as described in Chapter 2.

We then place the perfusion/flow system back to the incubator. After 20 hours, we repeat the same flow loading test. It is amazing that HUVECs restore their ability to release ATP again. This is quite an interesting result, telling us it would take a long time for cells to regain the sensitivity to shear stress.

3.5 Discussion

A perfusion/flow system is designed and fabricated for cell culture and flow loading test later on. It integrates the cell culture and flow tests into one single chip. The most distinguished advantage of such a system is its convenience. The cost is also low and it is disposable after each use. However the most challenging part in using the

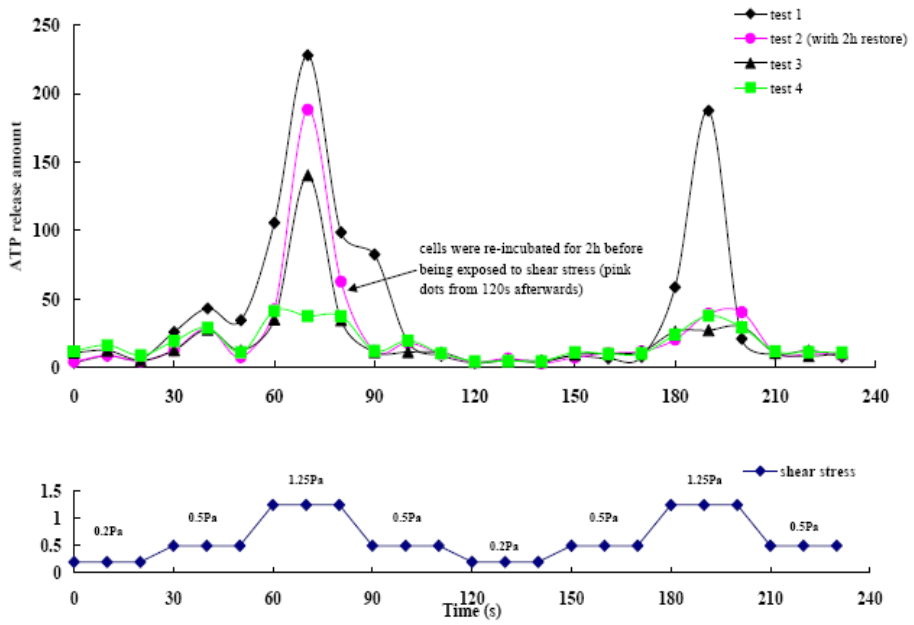

Figure 3.4: Shear-stress-induced ATP release from HUVECs. Time-varying shear stress is applied for about 4 minutes. Cells give a graded response to increased shear stress. However, when the same pattern of shear stress is applied for a second time, HUVECs are not able to give a response as strong as previously. Cells would restore the ability to release ATP after incubation for another 20 hours, as indicated by the rounded dots.

perfusion/flow system lies in the dynamic cell culture. The diameter and length of the winded channels should be calculated carefully to generate a desired resistance.

Chapter 4

Control of Extracellular ATP Level on Vascular Endothelial Cells Surface via Shear Stress Modulation

A good mathematical model could provide the description of a given system in great detail. In Chapter 2, we have put a lot of efforts in building and modifying such models. We then conduct the cell experiments to verify and rank these models by their prediction accuracy, as discussed in Chapter 3. However, the true value of mathematical modeling should be far beyond merely giving a perfect account of the events of our interest after rounds of polish based on simulation results and experimental data.

For control engineers, they always apt to intervene the system so that it would run in the fashion they desire. The mathematical model, to them is just like a road map, with which engineers would plan their routes to the destination (if it is within reach) more effectively. The ultimate goal of our work is to affect VECs response by adjusting external stimuli. In this chapter, we utilize the conventional PID controller to regulate ATP level on VECs surface. Three types of desired ATP level profiles including constant, square wave and sinusoid are obtained by regulating the wall shear stress under this PID control. The systematic methodology employed in this chapter to model and control ATP release from VECs via adjusting external stimulus opens up a new scenario, where quantitative investigations can be carried out for the sake of controlling specific cellular events.

4.1 Overview: Why the Regulation of Extracellular ATP is Physiologically Important

ATP has been widely accepted as a ubiquitous molecule regulating both intracellular and extracellular cell functions (Khakh & North [2006]). Compared with its intracellular role, known as "universal energy currency" for living cells, extracellular ATP regulation might be less well known and the mechanisms revealing how ATP transmits information between cells are more complicated. This is partly because ATP, confined to its size and charge, can not cross the cell membrane via simple diffusion.

In the past few decades, much effort has been devoted to investigating ATP release mechanism in various kinds of cells including excitable cells (e.g. neurons) and non-excitable cells like vascular endothelial cells (VECs) (see (Bodin & Burnstock [2001b]) for review). Studies (Bodin *et al.* [1991]; Milner *et al.* [1992]) demonstrated that VECs release ATP mostly under mechanical stimulation such as hemodynamic forces. This can be easily understood due to VECs' special location between the flowing blood and the vascular wall. Continuously exposed to the blood flow, VECs have been experiencing shear stress whose magnitude is much larger than those exist in other tissues and as a consequence, VECs have evolved to possess such mechanically-related response. Once the flow-induced ATP is transported to the extracellular space, it will in turn bind to the purinoceptors like P2X and P2Y on VECs surface (Bodin & Burnstock [2001b]; Ralevic & Burnstock. [1998]), which induces extracellular calcium influx and intracellular calcium release from cytosolic calcium stores Yamamoto *et al.* [2003]. As a result, vasodilators such as NO and prostacyclin (PGI_2) are elicited to release, which increase blood flow and oxygen delivery to the hypoxic tissue (Yamamoto *et al.* [2003]).

However, there still remain many questions incompletely understood in the process mentioned above. What's the quantitative relation between shear stress and ATP release? How will the extracellular ATP affect the signalling process? Does it depend on the magnitude or changing rate of ATP concentration, or both? Furthermore, how to compensate or impair ATP release for the purpose of medical treatment? In this thesis, we are trying to solve some of these puzzles, which are closely related to the flow-induced ATP release process, from a mathematical perspective. We believe this quantitative analysis will facilitate our future investigations into the downstream ATP-regulated reactions like intracellular calcium dynamics described above and thus be beneficial for decision making in medical treatment.

In this chapter, we would like to propose a new dynamic model, where both desensitization and re-activation are incorporated. Unlike the three models we have already

presented in Chapter 2, where shear stress is considered to induce ATP release directly, here we assume it is the flow-induced-deformation on cell that triggers ATP release, which is more physiological plausible (Wan *et al.* [2008] for the newly discovered mechanism for deformation-induced ATP release from red blood cells). Therefore, a subsystem describing the relation between shear stress and cell deformation is involved in our new model. Comparative studies are then conducted to demonstrate the advantage of the new dynamic model over the others by investigating the VECs responses under steady and pulsatile flow.

After the mathematical model is constructed, a conventional PID controller is applied to modulate ATP concentration at VECs surface such that it can follow a prescribed output. This is the first time that feedback, i.e., the error information between the prescribed extracellular ATP concentration and the real one, is utilized to adjust the shear stress exerted on VECs for a specific control aim, i.e., constant, square wave and sinusoid tracking.

The rest of the chapter is arranged as follows. The mathematical model for cell-deformation-induced ATP release is developed first. The model parameters are obtained by fitting the model-generated samples with the experimental data (Yamamoto *et al.* [2003]), where the optimization algorithm is employed in a recursive way. The following section presents the PID control procedure. Simulation results and discussion are demonstrated as well.

4.2 Model Modification: Cell-deformation-induced ATP Release

To describe ATP distribution in the flow chamber, the diffusion-convection equation in Chapter 2 is utilized except that the boundary condition for bottom surface is now expressed as

$$\begin{aligned} D \left.\frac{\partial c}{\partial y}\right|_{y=0} &= \left.\frac{V_{\max} c}{K_{\mathrm{m}} + c}\right|_{y=0} - S_{\mathrm{ATP}}(\varepsilon, t) \\ &\equiv -S_{\mathrm{net,ATP}}, \end{aligned} \tag{4.1}$$

where $V_{\max}$ is the maximum enzyme reaction velocity for ATP hydrolysis and K_{m} is the Michaelis constant for the enzyme, which are the same as those in Chapter 2. $S_{\mathrm{ATP}}(\varepsilon, t)$ is the source term for endothelial deformation induced ATP release, which depends not only on ε, the overall deformation of VECs, but on time t as well. The average net

ATP release rate $S_{\text{net,ATP}}$ against time t under different shear stresses τ_w (thus different cell deformations ε) can be measured by *in vitro* cell experiments (Yamamoto *et al.* [2003]). We notice that it is not the shear stress but the cell deformation triggered by shear stress that induces ATP release from VECs. Though this modification seems mathematically trivial, it, however is more physiologically plausible, as will be shown in the following subsections.

4.2.1 Two-step Mechanism for ATP Rlease

Once the flow is applied in the chamber, cell deformation occurs due to the direct interaction between the flowing medium and VECs surface. In this process, VECs can be modelled as a Kelvin body, with standard linear solid behavior (Barakat [2001]). The following equation describes the relationship between the body deformation, denoted as ε and exerted force, which is the wall shear stress τ_w in our case.

$$\zeta\left(1+\frac{k_1}{k_2}\right)\dot{\varepsilon}+k_1\varepsilon=\tau_w+\frac{\zeta}{k_2}\dot{\tau}_w, \tag{4.2}$$

where k_1, k_2 are the spring constants and ζ is the viscosity coefficient of the Kelvin body. As illustrated by Fung (Fung [1981]) and Barakat (Barakat [2001]), the initial condition for a Kelvin viscoelastic body is given by

$$\left.\frac{1}{k_2}\tau_w\right|_{t=0}=\left.\left(1+\frac{k_1}{k_2}\right)\varepsilon\right|_{t=0}. \tag{4.3}$$

Although the cellular response of VECs to external mechanical stimuli has been an active research subject since late 1980s (Ando *et al.* [1988, 1991]), the precise mechanism of flow-induced ATP release still remains obscure. In consideration of the widely accepted mechanisms proposed by Bodin and Yamamoto(Bodin & Burnstock [2001b]; Yamamoto *et al.* [2007]), we assume that ATP release depends on (1) the magnitude of cell deformation and (2) the activation level of various ATP pathways. Thus we have

$$S_{\text{ATP}}(\varepsilon,t)=\hat{p}_1\hat{p}_2, \tag{4.4}$$

where the state variable, $\hat{p}_1$, summarizes the effect of deformation-elicited ATP release pathways, and the state variable, $\hat{p}_2\in[0,1]$ describes the activation level of the various ATP release pathways, satisfying the following equations

$$\frac{d\hat{p}_1}{dt}=-\frac{\hat{p}_1}{\hat{\tau}_1}+f(\varepsilon), \tag{4.5}$$

$$\frac{d\hat{p}_2}{dt} = -\frac{\hat{p}_2}{\hat{\tau}_2} + \hat{\lambda}\left|\frac{d\varepsilon}{dt}\right|, \tag{4.6}$$

where $\hat{\tau}_1$, $\hat{\tau}_2$ are time constants and $\hat{\lambda}$ is the re-activation coefficient; $f(\varepsilon)$ is a function of cell deformation and it is proposed to take the following form,

$$f(\varepsilon) = \hat{a}_1 + \frac{\hat{a}_2\varepsilon}{\hat{a}_3 + \varepsilon}. \tag{4.7}$$

where $\hat{a}_1$, $\hat{a}_2$ and $\hat{a}_3$ are model parameters.

The initial conditions for p_1 and p_2 are

$$\hat{p}_1(0) = 0, \tag{4.8}$$

$$\hat{p}_2(0) = 1, \tag{4.9}$$

implying initially there is no ATP release but all possible pathways are in activated status.

The whole process for deformation-induced ATP release is governed by Eqs.(4.2), (4.5) and (4.6), where $k_1, k_2, \zeta, \hat{a}_1, \hat{a}_2, \hat{a}_3, \hat{\tau}_1, \hat{\tau}_2$ and $\hat{\lambda}$ are the model parameters to be determined by experimental data (Yamamoto *et al.* [2003]), as will be elaborated in the following subsection.

Remark 6. *It is worth noting that $f(\varepsilon)$ bears the same form as that of the well known Hill function, widely used in modelling cell functions in biochemistry, which captures the common characteristic of many cellular responses to stimuli that the intensity of the response would increase with the intensity of the stimulus, but with a saturation point. The offset term, $\hat{a}_1$, which is usually very small, is included to take into account possible natural ATP release; for instance, VECs always weakly release ATP.*

Remark 7. *The purpose of including the state variable $\hat{p}_2$ in the dynamic model is to capture the characteristics of "desensitization" and "re-activation" of all possible pathways through which ATP can be transported. The desensitization rate is governed by time constant $\hat{\tau}_2$ and the re-activation level is assumed to be proportional to the magnitude of deformation rate. Despite the fact that currently there is no direct experimental evidence to show these two mechanisms in the deformation-induced ATP release process, we speculate that they would occur in this event since it is such a common phenomenon in many cellular responses of biological systems.*

4.2.2 Model Parameter Identification

Yamamoto and her co-workers (Yamamoto *et al.* [2003]) published their experimental data about the average net ATP release rate $S_{\text{net,ATP}}$ (defined in Eq.(4.1)) against time t using HPAECs exposed to a stepwise increasing fluid shear stress ($0 \rightarrow 0.3 \rightarrow 0.8 \rightarrow 1.5$Pa). The model parameters are computed by minimizing the difference, E, of experimental points and corresponding sample points generated by our model.

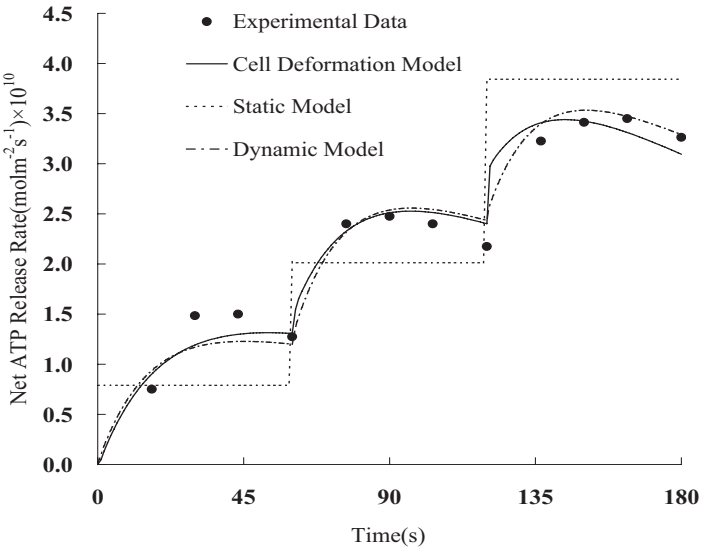

Figure 4.1: Comparison between experimental and corresponding model predicted average net ATP release rate S_{ATP} against time t. Experimental data is collected from Yamamoto *et al.* [2003]; cell deformation model and dynamic model refer to current model in this chapter and the original dynamic model in Chapter 2; static model refers to the work conducted by John & Barakat [2001].

$$E(k_1, k_2, \zeta, \hat{a}_1, \hat{a}_2, \hat{a}_3, \hat{\tau}_1, \hat{\tau}_2, \hat{\lambda}) = \sum_{n=1}^{N} \left(S_{\text{net,ATP-predicted}}(n) - S_{\text{net,ATP-exp}}(n)\right)^2, \quad (4.10)$$

where N is the total number of experimental samples, $S_{\text{net,ATP-exp}}(n)$ is the value of the nth sample point. $S_{\text{net,ATP-predicted}}(n)$ is the model-predicted net ATP release rate expressed as

$$S_{\text{net,ATP-predicted}} = S_{\text{ATP}}(\varepsilon, t) - \frac{1}{L}\int_0^L \frac{V_{\max} c|_{y=0}}{K_{\text{m}} + c|_{y=0}}\, dx, \quad (4.11)$$

The calculation of Eq.(4.11) should take into account the governing equation described in Chapter 2 with the corresponding boundary and initial conditions. The average value in the direction of x is taken in Eq.(4.11) since the experimental measurements of the net ATP release rate, $S_{\mathrm{net,ATP-exp}}(n)$, were obtained as averaged values in the experiments.

In this case, we divide the 9 parameters into 2 groups (deformation and release group) and apply the optimization algorithm (sequential quadratic programming method by Nocedal & Wright [1999]) in a recursive manner, which means for each recursive iteration, only one group of parameters are being optimized while the remaining ones are kept still. By doing so, the number of tuned parameters is reduced in each iteration and thus enhancing the effectiveness and accurateness of the adopted algorithm. Besides, we choose various sets of starting points to avoid being trapped in local minima. This has been proved effective from Fig 4.1, where the predicted net ATP release rate shows good consistence with the experimental data. We also show the fitting results of other existing ATP release models for comparison and it is convinced a dynamic ATP release model is necessary to capture the essential characteristics of ATP release. Table 2 lists all the optimized model parameters used in this chapter.

4.3 PID Control for Extracellular ATP Level

In this section, we focus on the generation of a desired shear stress profile with which, the average extracellular ATP concentration can be maintained at a constant level or track a given reference like square wave and sinusoid. The dynamics of ATP transportation in the chamber is governed by a partial differential equation, which is not only nonlinear but infinite dimensional as well. Control of finite dimensional nonlinear systems has been a subject of research for several decades but no single approach has been found to be satisfactory for all situations. In this case, the problem is even more challenging by compounding the fact that the system is infinite dimensional.

Although the dynamic system appears very complex, it is a truism in control practice that the simplest controller which satisfies all the constraints while meeting performance specifications is the one that should be chosen. This is because simplicity of the controller also generally implies robustness. It is even more true as the complexity of the system to be controlled increases. In view of the complexity of the ATP dynamics, it is proposed, that, before proceeding to use more sophisticated nonlinear controllers, simpler controllers should be considered first. In particular, PID controllers should be simulated first to see whether the tracking task could be achieved. Thus, the shear

Table 2: Parameters for Cell-deformation-induced ATP Release Model

Para	Unit	Value	Remark
L	m	0.025	
h	μm	200	
μ	N s m^{-2}	9.45×10^{-4}	
D	m^{2}s^{-1}	2.36×10^{-10}	
K_{m}	μM	475	
$V_{\max}$	mol m^{-2}s^{-1}	0.8×10^{-6}	
k_1	Pa	48.5	cell deformation model
k_2	Pa	100.8	
ζ	Pa s	999.7	
$\hat{a}_1$	mol m^{-2}s^{-2}	0	ATP release model;
$\hat{a}_2$	mol m^{-2}s^{-2}	5.74×10^{-11}	$\hat{a}_1$ is set zero as the optimized
$\hat{a}_3$		0.007	value can be ignored in $f(\varepsilon)$
$\hat{\tau}_1$	s	8.78	
$\hat{\tau}_2$	s	168.6	
$\hat{\lambda}$		32.27	

Table 3: Controller parameters for constant, square wave and sinusoid tracking

	constant	square wave	sinusoid
K_p (Pa m^3mol^{-1})	2.09×10^4	2.14×10^4	2.0×10^4
K_i (Pa $m^3mol^{-1}s^{-1}$)	1.0×10^2	1.13×10^2	5.0×10^2
K_d (Pa m s^3mol^{-1})	4.42×10^4	4.49×10^4	7.0×10^4
bias (Pa)	7.2×10^{-2}	7.0×10^{-2}	0

stress (control input) has the form of

$$u(t) = \tau_w(t) = \text{bias} + k_p e(t) + k_i \int_0^t e(t)dt + k_d \frac{de(t)}{dt}, \quad (4.12)$$

where k_p, k_i, k_d and bias are the controller parameters and $e(t)$ is the error signal, defined as

$$e(t) = \text{ref}(t) - \frac{1}{L}\int_0^L c(x, y; t) \mid_{y=0} dx, \quad (4.13)$$

where $\text{ref}(t)$ is the reference signal, denoting the average ATP concentration on the cell surface.

The ITSE criterion, which is expressed as

$$\text{ITSE} = \int_0^t te^2(t)dt \quad (4.14)$$

is employed to be the cost function to be minimized in order to obtain the control parameters. Table 3 lists the corresponding gains for different control tasks such as set point tracking, square wave and sinusoid tracking.

4.4 Simulation Studies

4.4.1 System Response Under Step-wise and Pulsatile Flow

Fig 4.2 demonstrates the predicted dynamic behaviors of the average extracellular ATP concentration at VECs surface under stepwise manner shear stress stimulation. Parameters used for cell deformation model can be found in Table 2 and those for dynamic and static models are listed in Table 1.

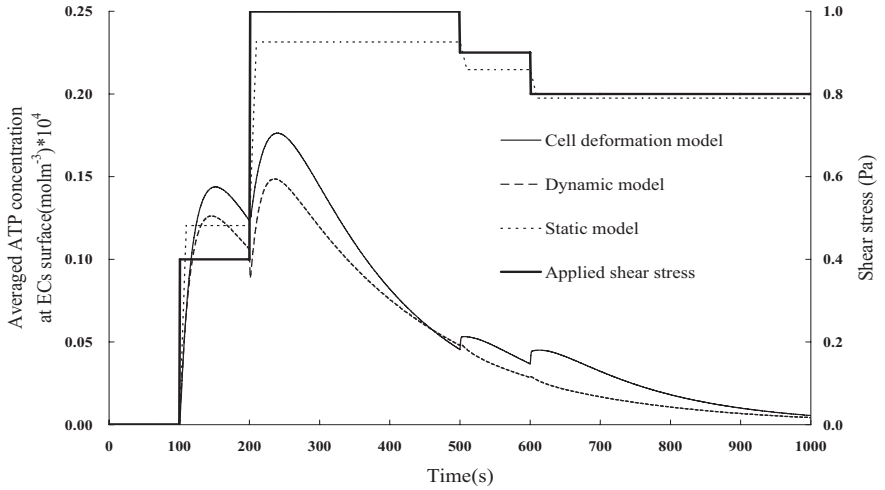

Figure 4.2: Comparison among cell deformation, original dynamic (see Chapter 2) and static (see John & Barakat [2001]) model-predicted extracellular ATP concentration at VECs surface against time from the onset of steady fluid shear stress in a stepwise manner ($0 \rightarrow 0.4 \rightarrow 1 \rightarrow 0.8 \rightarrow 0.9$Pa).

It can be readily seen that the average ATP concentrations predicted by our two models (cell deformation and original dynamic models) are indeed dramatically different from that predicted by the static model. In particular, after VECs being activated for a long time (300-500s) by a step shear stress 1Pa, the static model predicts a stable concentration while the our models predict a gradually decreasing response. There are some indirect experimental evidences, such as the experiment carried out on HUVECs by Bodin & Burnstock [2001a]. It is clearly manifested in the Fig 1 of the paper Bodin & Burnstock [2001a], that being activated by a small step shear stress for one period and then a larger step shear stress for a much longer period, the ATP concentration initially increases to a maximum level and then gradually decreases, which agrees qualitatively with the predictions made by our two dynamic models.

We intentionally make the shear stress decrease from 1 to 0.9Pa at 500s and then to 0.8Pa at 600s in order to see different behaviors of ATP concentration predicted by the cell deformation and the dynamic models. The ATP concentration predicted by the dynamic model does not have an obvious response to the decreased shear stress. However, in the cell deformation model, there is a sudden jump of ATP concentration corresponding to the sudden decrease of shear stress. It is not difficult to understand the different responses as in the cell deformation model, re-activation mechanism is considered and any change in cell formation will stimulate certain pathways to activated

status. However, direct experimental evidence is needed to help us judge which of the two predictions is closer to the real case.

Despite the fact that none of the real experiments related to flow-induced ATP release on VECs have been conducted for pulsatile flow, further numerical comparison studies are carried out for ATP concentration prediction as this is more physiologically relevant to human VECs. Fig 4.3 displays the dynamic behavior of the extracellular average ATP concentration at VECs surface from the onset of pulsatile fluid shear stress.

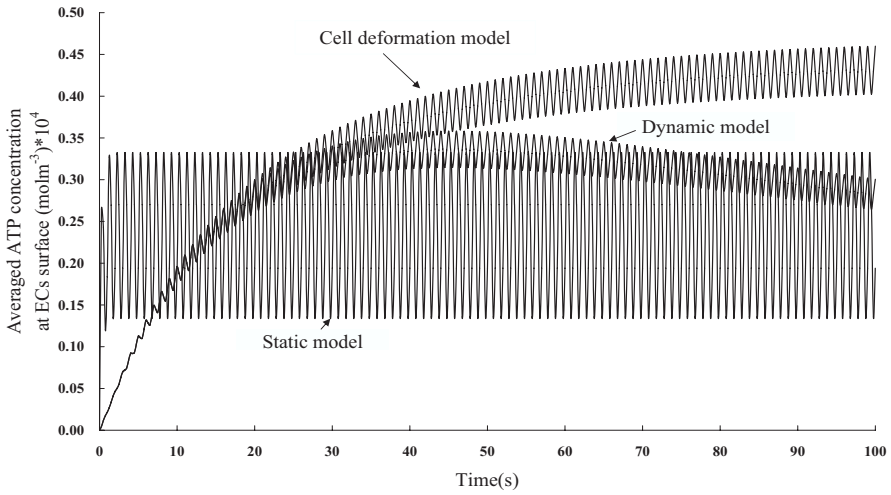

Figure 4.3: Comparison among cell deformation, original dynamic (see Chapter 2) and static (see John & Barakat [2001]) model-predicted extracellular ATP concentration at VECs surface against time from the onset of pulsatile fluid shear stress $\tau_w = 1+\sin(2\pi t)$.

It is noticed from Fig 4.3 that, during the initial period right after the onset of pulsatile flow, the dynamic behaviors of the average ATP concentration at endothelial surface predicted by our two dynamic models are quite different from that predicted by the static model. However, after around 40s, the cell deformation, original dynamic and static models predict a very similar characteristic of the ATP concentration at endothelial surface: an oscillation with the same period of 1s as that of the pulsatile flow, even though the predicted magnitudes of oscillations are quite different. It is also noticed that the magnitude of the oscillation predicted by the dynamic model gradually decreases with time in the long run, due to the effect of "receptor desensitization", which usually occurs to a constant stimulus. Therefore the cell deformation model-predicted ATP concentration seems to be more reasonable in face of a time-varying sinusoidal shear stress. As can be seen from Fig 4.3, the magnitude of its oscillation tends to stay

within a fixed range.

4.4.2 System Response under PID Control

Fig 4.4 and Fig 4.5 demonstrate the average ATP concentration at VECs surface under PID control, when the reference are constant and square wave, respectively.

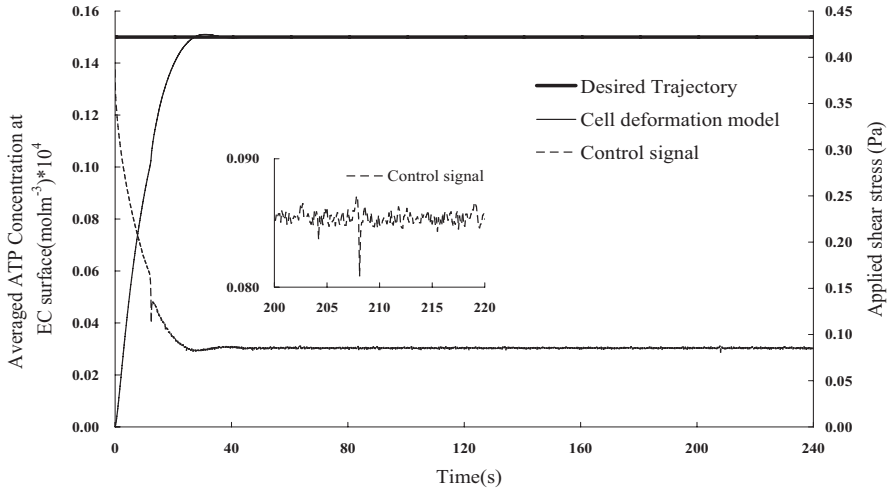

Figure 4.4: Constant tracking for extracellular ATP under ITSE-based PID controller and applied shear stress.

It seems the conventional PID controller works effectively for constant tracking since just after 40s, the extracellular ATP concentration can be maintained at the constant level. In the very beginning, a quite large flow rate should be applied to activate deformation-induced ATP release and then the flow rate is tuned to drop gradually. It seems very confusing that the decreased flow rate would yield the increased ATP concentration at VECs surface. However this is true since it is easier for ATP to accumulate at cell surface when the flow rate is small. Though the release amount is reduced, it is compensated by the impaired convection. One interesting phenomenon lies in the noisy input signal after 40s (see the amplified signal in Fig 4.4). The noise in fact helps to maintain all possible ATP pathways in active states and thus guarantees continuous ATP release.

For the square wave tracking task, a very similar input profile is applied. It is worth noting that manual regulation is involved in order to reduce extracellular ATP concentration, as can be seen from the control signal curve (dashed line in Fig 4.5) in the periods of 240-280s and 900-940s. In these intervals, we apply the minimum shear

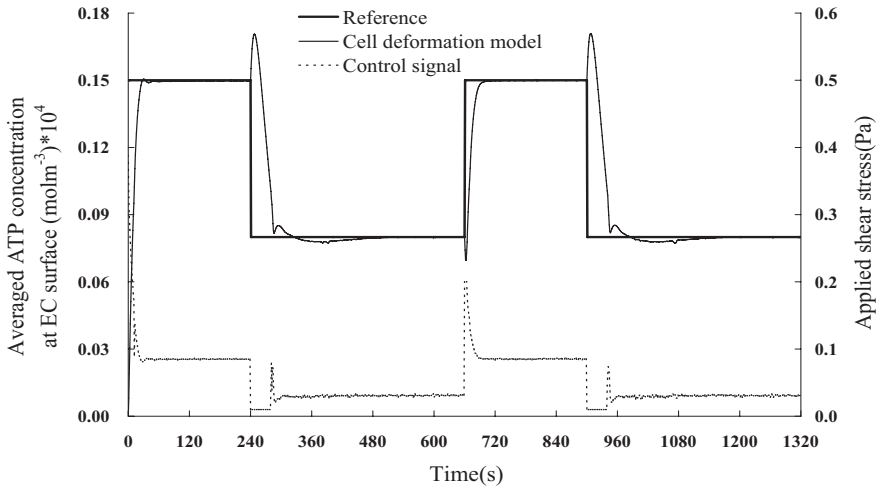

Figure 4.5: Square wave tracking for extracellular ATP under ITSE-based PID controller and applied shear stress.

stress (0.01 Pa) for 40s and let extracellular ATP concentration drop by itself.

We then try to track a sinusoidal reference with this simple PID controller and the system performance is shown in Fig 4.6. Unfortunately, the PID controller seems to lose effect: the system output deviates a lot from the reference signal, indicating that more sophisticated control schemes are required for tracking a dynamic reference such as sinusoid.

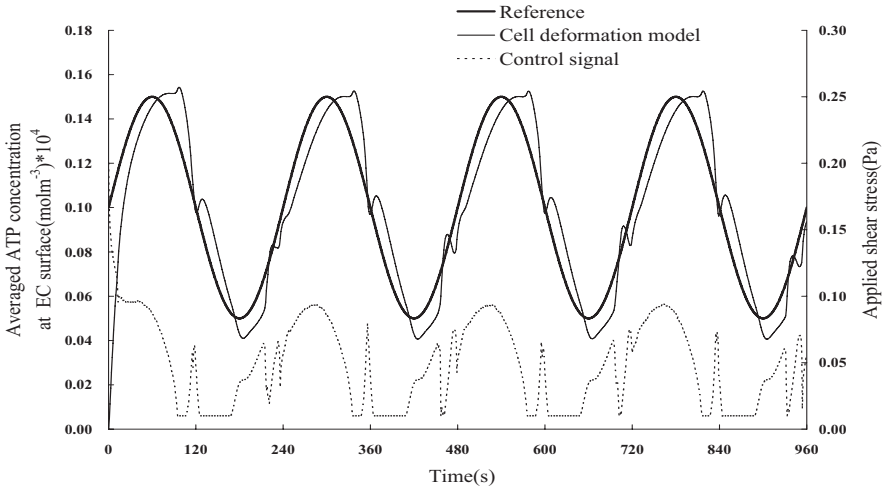

Figure 4.6: Sinusoid tracking for extracellular ATP under ITSE-based PID controller and applied shear stress.

4.5 Discussion

In this chapter, a mathematical model of cell-deformation-induced ATP release from VECs is proposed first to quantify the relation between external stimulus (the shear-stress-induced deformation) and the response of VECs (ATP release). Simulation studies are then conducted to predict the VECs responses to stepwise and pulsatile flow, respectively. With the incorporation of cell deformation model, the established plant would behave more like a real biological system. It has been reported that cells exposed to flow can sense the shear stress and deform accordingly. Therefore deformation, rather than shear stress is more likely to activate ATP release directly. Comparisons are made among the static, dynamic and cell deformation models. From the simulation results, the two dynamic models predict very different system behaviors to the static one, though some subtle differences also exist in these two models. Direct experiments are necessary to verify which of them is more accurate.

Once the model is completely obtained, the PID control is applied to the system. It is demonstrated to be effective for maintaining extracellular ATP at a constant level or for driving it to follow a desired square wave. However, perfect tracking of more complicated reference signals like sinusoid requires more advanced and sophisticated model-based controller design, which is very challenging due to the nature of the problem itself. As far as we know, this is the first time that a systematic method is employed to modulate external stimulus to VECs cultured *in vitro* to investigate whether cells would behave in a desired manner, which, together with the cell deformation model, constitutes the main contribution.

Unfortunately, the implementation of such PID scheme in a real plant might not give us as good results as shown in this chapter. This is mainly due to the fact that VECs would be strongly adaptive to the stimulation of shear stress, as indicated in Chapter 3. We still keep this piece of simulation work here as part of the whole thesis as it has shown the validation of PID controller in systems governed by partial differential equations.

Future work on extracellular ATP regulation can be conducted along two lines. On one hand, more sophisticated scheme should be proposed to improve the tracking performance. On the other hand, the experiment on reactivating membrane receptors must be done to (1) obtain more biological evidences for building a better model and (2) more importantly to provide hints for understanding how the dynamic behavior of extracellular ATP profile would affect the downstream reactions and what kind of profile is preferred for certain physiological or medical purpose.

Chapter 5

Regulation Intracellular Calcium Dynamics via Shear Stress and ATP

We now shift our focus back to the cell experiment regarding "shear stress → ATP release → calcium dynamics" pathway. As verified by our own data, VECs would release ATP under mechanical stimulus like shear stress. The receptor desensitization phenomenon exists and it would take about 20 hours for HUVECs to restore this capacity. Though ATP release is fast and its amount is large, the short duration, or the strong desensitization makes the mission of short-term regulation ATP release almost impossible under current condition. That is why we only present some primary simulation studies on regulation of ATP level. With shear stress alone, the system seems uncontrollable.

How about the regulation of intracellular calcium dynamics? Shear-stress-induced ATP would directly bind to P2X receptors, leading to the calcium flux across VECs membrane. Extracellular ATP may also activate P2Y receptors, which consequently brings about stronger calcium response in the cytosol via opening the intracellular calcium store. To maintain the active response status of VECs, we introduce exogenous ATP, together with shear stress to boost calcium response. By carefully combining the two input signals, we generate letters "N", "U" and "S" with both open loop and closed loop control. Though the we know very little of how these "N", "U" and "S" profiles would affect downstream reactions, these results may indicate our capacity to intervene cell behavior as we know how to encode information in calcium response, which would have a profound impact to VECs functions.

In this chapter, we first give a brief overview of how intracellular calcium modulates its downstream reactions and finally affects cell functions. The calcium imaging experiment is demonstrated followed by. We then show some primary results on generating desired calcium signals, such as letters "N", "U" and "S". The last section concludes the whole chapter.

5.1 Overview

Calcium, as a ubiquitous second messenger found in almost all types of cells, has played an important role regulating various cellular functions. In human vascular endothelial cells, the dynamic behavior of cytosolic calcium, i.e., temporal/special variation of calcium concentration, will directly affect cell proliferation, synthesis and secretion of vaso-active factors like NO, and gene regulation. Therefore finding the way to encode useful information into calcium signaling process, that is to adjust the calcium dynamics via external stimuli, has become extremely meaningful.

In 1995, Gu and Spitzer (Gu & Spitzer [1995]) observed the frequency of Ca^{2+} oscillation would direct the differentiation of developing neurons. This was the first time the dynamic features of intracellular calcium attracted intensive interests of scientists. The information carried by calcium in terms of its concentration, distribution and other spatio/tempral characteristics, directs the life cycle even of a single cell. Berridge (Berridge [1997]) termed it as the AM and FM of calcium signaling, providing a engineering perspective for us to view cellular signaling. Dolmetsch and his colleagues reported in 1997 (Dolmetsch *et al.* [1997]) that the duration and amplitude of Ca^{2+} would also influence cell response. They correlated Ca^{2+} oscillation and gene expression in 1998 and found that oscillation would increase the efficiency and specificity of gene expression Dolmetsch *et al.* [1998]. Li *et al* synthesized inositol 1,4,5-trisphosphate (InsP3), the substance to increase calcium release from intracellular calcium store. Delivering InsP3 to cells, they found an optimal status of gene expression by adjusting the delivery fashion (Li *et al.* [1998]).

These early investigations encourage us to explore information encoding in calcium response via adjusting shear stress and exogenous ATP.

5.2 Experiment Setup

5.2.1 Cell Culture in Perfusion/Flow System for Ca^{2+} Imaging

The perfusion/flow system is utilized here for HUVECs and human pulmonary artery endothelial cells (HPAECs) growth. For Ca^{2+} imaging test, the perfusion/flow system is fabricated with two inlets, one for ATP free buffer medium and the other for medium containing high level of ATP. By adjusting the flow rates of the two inlets, we could generate input flow with different rate and ATP concentration. HUVECs from passage 4 to 6 while HPACECs from passage 7 to 10 are used in experiments. The detailed procedure of cell seeding and culture are described in Chapter 3. When cells reach 80% confluence, we start the imaging tests.

5.2.2 Construction of Flow Circuit

The flow circuit comprises two syringe pumps (Harvard Pumps), one fluorescence microscope, one charge coupled device (CCD) camera, one personal computer and the perfusion/flow system. The programmable pumps are used to generate different kinds of input signals to trigger the intracellular calcium response, which can be observed under microscope and captured by CCD camera for later analysis.

Pictures taken by CCD camera will be downloaded to the computer for analysis. In this experiment, we focus on the average intensity (represents intracellular calcium level) in the observation field. Based on the result, commands would send to pumps. By doing so, a closed flow circuit has been built.

5.2.3 Measurement of Intracellular Ca^{2+}

When cells reach 80% confluence in the perfusion/flow system, fresh Hanks balanced solution (HBSS) is filled in the reservoir to rinse the cells slowly. This is a essential procedure before loading the calcium indicator Fluo 3. After the rinse, calcium indicator is loaded to the system (4μM in HBSS solution) in dark. Incubate the cells at 30 degree for 20 minutes. Gently rinse the cells, introduce fresh HBSS and incubate for another 20 minutes.

When the perfusion/flow system is connected to the flow circuit, start the pump and rinse the cell slowly (shear stress less than 0.1Pa) to wash off the residuals such as Fluo 3 indicators in the chamber. Avoid long exposure of cells to lighting source as it would bleach the indicator and thus affect measurement. Be as cautious as possible

while connecting the perfusion system with the syringes. Air bubbles would destroy the whole test.

Pictures are taken by CCD camera every three seconds.

5.3 Some Primary Results on Intracellular Calcium Regulation

To optimize the microscope and camera settings (i.e., focus plane, the open percentage of the light gate, exposure time, ISO and etc), we first culture HPAECs in the perfusion/flow system as its calcium response to shear stress is strong and could be easily detected.

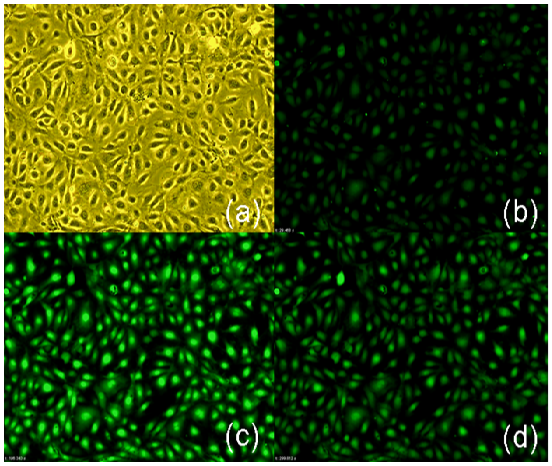

Figure 5.1: Intracellular calcium response to shear stress in HPAECs. HPAECs about 80%-90% confluent in perfusion/flow system right before calcium imaging. Picture taken via phase contrast set up (a). HPAECs under fluorescence microscope before flow (b). Picture taken during the flow loading process (c). Picture taken after the test (d).

As can be seen from Fig 5.1, cells maintain normal morphology after indicator loading. The yellow background is caused by the FITC cubic mirror in the microscope. When the cells are exposed to the excited light source, we can see from (b) that the green fluorescence given off by the cells even without shear stress or ATP stimulation. This indicates the free intracellular calcium level when cells are at rest status. Generally speaking, ISO could be reduced in this case until the whole screen is black. This is because high ISO would bring much noise, causing measurement error in the exper-

iment. We take one picture (c) when cells give a very strong response to shear stress. It can be clearly seen from the figure that almost all of the cells in the observation field have responded to shear stress. The fluorescence they give off make them visible.

We finally do not choose HPAECs for investigation as they are too active to shear stress. Usually shear stress at about 0.5Pa could initiate the response and once it starts, we currently could not terminate it even the flow has been stopped. We choose HUVECs and observe its calcium response under the stimulation of shear stress and ATP. This is because HUVECs release very limited amount of ATP themselves. They are mild and seem to be controlled easily.

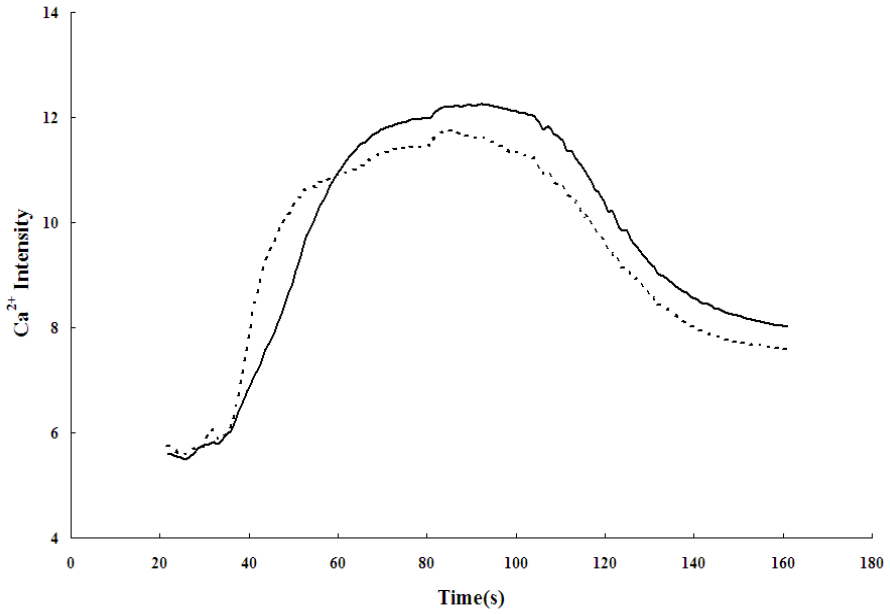

Figure 5.2: Intracellular calcium response of HUVECs to a combined shear stress and ATP stimulation. The average fluorescence intensity is plot. By carefully combine the two input signals, we could increase the calcium level and make it hold for about 60 seconds. The flow pattern used to generate such shape is as follows: 0-20s, rinse, ATP free, 0.5ml/min; 20-50s, 250-500nM ATP, 1ml/min; 50-74s, 500-800nM ATP, 1ml/min; 74-98s 1μM ATP, 2ml/min; 98-119s, ATP free, 1ml/min; 119s- flow stops.

Fig 5.2 plots two calcium response curve under a combined shear stress and ATP stimulation. In the first 20 seconds, we apply slow flow to rinse the cells. The next 30 seconds, we increase a little bit ATP level and flow rate to initiate the pathway. Not like HPAECs, HUVECs would not release large amounts of ATP, we then decide to supplement ATP in the very beginning. To avoid desensitization, for the following

60 seconds, more ATP is added and shear stress is also increased so as to maintain the calcium level in the cells. When we use ATP free medium to flush the cells for 20 seconds, calcium level drops gradually. This proves that exogenous ATP is an important source for intracellular calcium response.

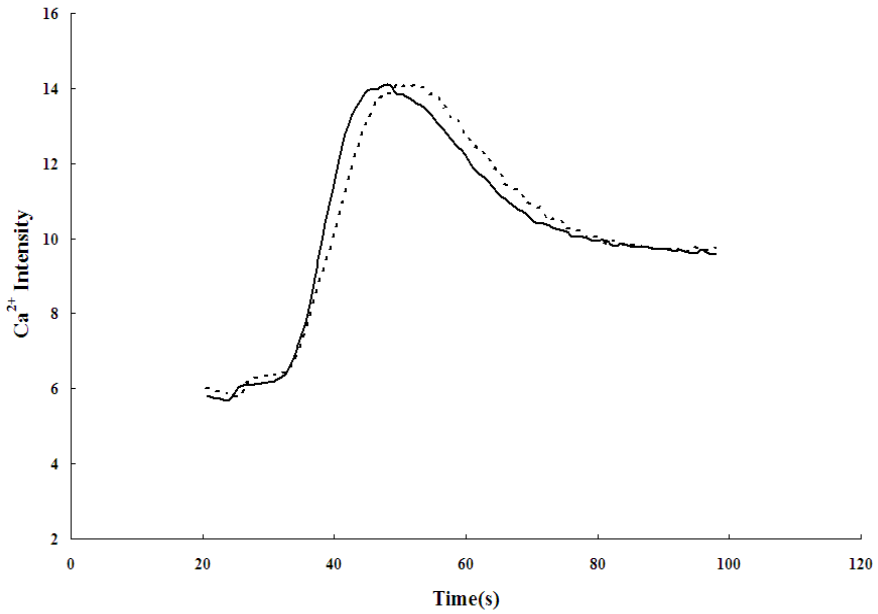

Figure 5.3: Intracellular calcium response of HUVECs to a combined shear stress and ATP stimulation. The average fluorescence intensity is plot. By carefully combine the two input signals, we could increase the spike like calcium profile. The duration of calcium level staying at high level is shortened. The flow pattern used to generate such shape is as follows: 0-20s, rinse, ATP free, 0.5ml/min; 20-40s, 2μM ATP, 1ml/min; 40-100s, ATP free, 1ml/min; 100s- flow stops.

Fig 5.3 plots another simple shape (spike-like calcium profile) by adjusting the combination of shear stress and ATP a little. Rinse process is kept as it is essential for each test. To generate a spike-like pattern, we need to enhance HUVECs exposure to ATP and then remove ATP quickly. Hence in the following 20 seconds, we apply a very high ATP level and at the same time increase a little the flow rate so that ATP would have more chance to bind to the receptors. For the remaining time, ATP free buffer is used to wash off ATP. We keep the flow rate unchanged in order not to reactivate shear-stress-sensitive receptors. Otherwise, calcium level will not drop to the basal line so fast.

We could now conclude that the duration and the magnitude of average intracellular

calcium could be regulated by carefully design the input signals. We know very little how these two patterns would affect the downstream reactions as we observe calcium dynamics only. We leave this as an open problem for future investigation.

5.4 Generation of "NUS"

In this section, we would like to regulate intracellular calcium level via adjusting shear stress and ATP. The profile of the average Ca^{2+} could track letters "N", "U" and "S", representing " National University of Singapore". These three letters are generated via both open loop control (i.e., a prescribed command is given) and closed loop control, which would update input command with feedback.

We use HUVECs instead of HPAECs in calcium regulation experiment mainly because ATP release from HUVECs are very limited thus could be ignored in regulation process. This makes it simple to design the control commands.

5.4.1 Open Loop Control System

In open loop system, pictures taken by the CCD camera would not be further analyzed to generate input signals. The control commands, i.e., the profiles of shear stress and ATP are set before the tests and they rely a lot on experiences.

The solid line with squares in Fig 5.4 is the average intensity of the light given off by free intracellular calcium ion (we will use calcium intensity for simplicity in the following context). Cells are rinsed by ATP free buffer for 20s before images are taken. The prescribed command is as follows. In the first 30 seconds, cells are flushed by buffer containing 250-500nM ATP at the flow rate of 1ml/min. For the next 24 seconds, we double the ATP level (500-800nM ATP, 1ml/min) to boost calcium increase. When the calcium level approaches to the peak value (estimated before the test), more ATP is supplemented to 2μM and flow rate elevated to 2ml/min. At this stage, receptor desensitization may occur. To maintain the calcium level, it is necessary to adjust input stimuli so that receptors might be reactivated. Calcium level will drop if extracellular ATP is washed off. In the last stage, we gently wash the cells with ATP free buffer. The tracking performance is acceptable as errors in biological system are usually large.

The letter "U" is composed of two spikes, generated by two strong but fast stimuli. HUVECs are exposed to buffer with high ATP concentration for 20 seconds with very gentle flow. Then ATP free buffer is used to remove the residual so that calcium level would decrease. For the second spike, the stimuli should be stronger due to the fact that cells are adaptive to their environment.

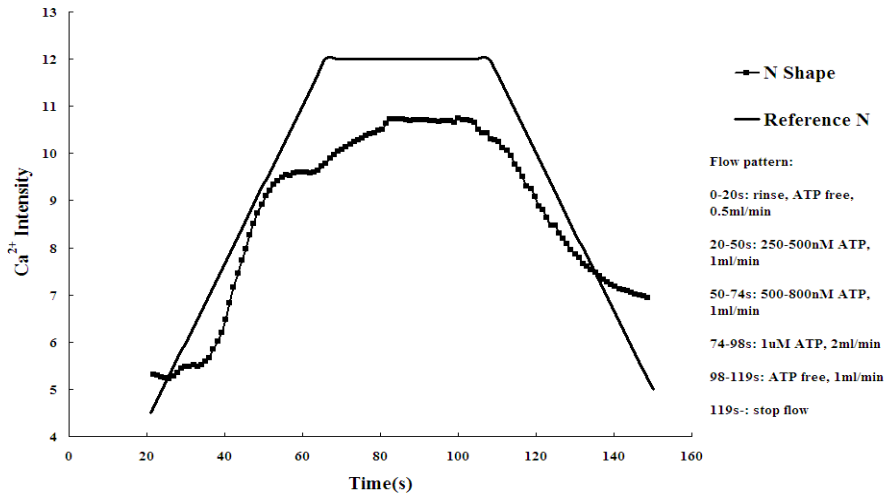

Figure 5.4: "N" shape. The bold solid line is the reference letter "N" and the line with squares is the average intensity of the light given off by free calcium. HUVECs are rinsed by ATP free buffer gently for 20 seconds. For the next 30 seconds, we apply buffer containing 250-500nM ATP to flush the cells at a moderate flow rate (1ml/min) so that intracellular calcium level would climb up. More ATP (500-800nM) is supplemented for the following 24 seconds. However we do not elevate the shear stress level as the stimulation is sufficient. We then increase ATP level (1μM) and flow rate (2ml/min) simultaneously to maintain calcium level. At this stage, receptor desensitization might happen. Finally, we stop the flow and set cells at rest status. The calcium level would drop.

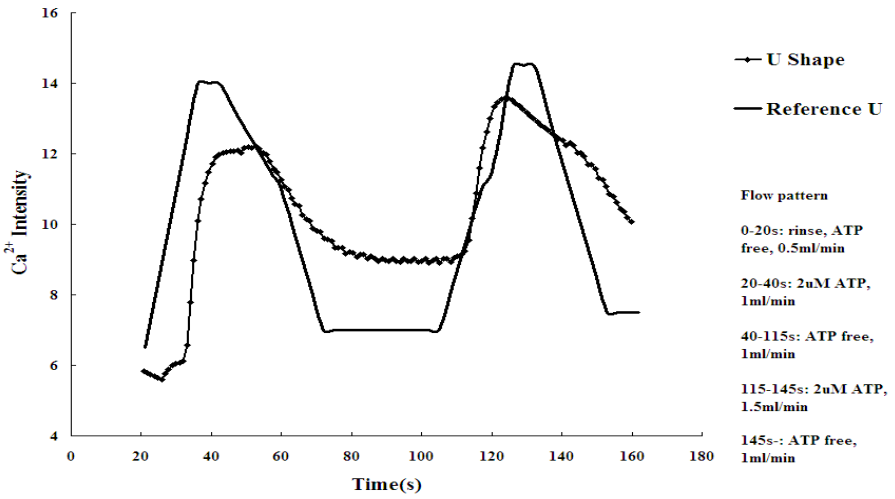

Figure 5.5: "U" shape. The bold solid line is the reference letter "U" and the line with dots is the calcium intensity. HUVECs are rinsed gently with ATP free buffer at the flow rate of 0.5ml/min for 20 seconds. For the next 20 seconds, we apply buffer containing 2μM ATP to flush the cells at a moderate flow rate (1ml/min) so that intracellular calcium level would suddenly jump to a high level. As the "U" shape is composed of two spikes, a sudden drop is required next. In order to remove the remaining ATP on cell surface, we apply ATP free buffer for 75 seconds. The flow rate is set as 1ml/min. To trigger the second spike, we increase the flow rate to 1.5ml/min and ATP to 2μM and such process lasts for 30 seconds. ATP free buffer is utilized again to remove residual ATP and the calcium level drops gradually.

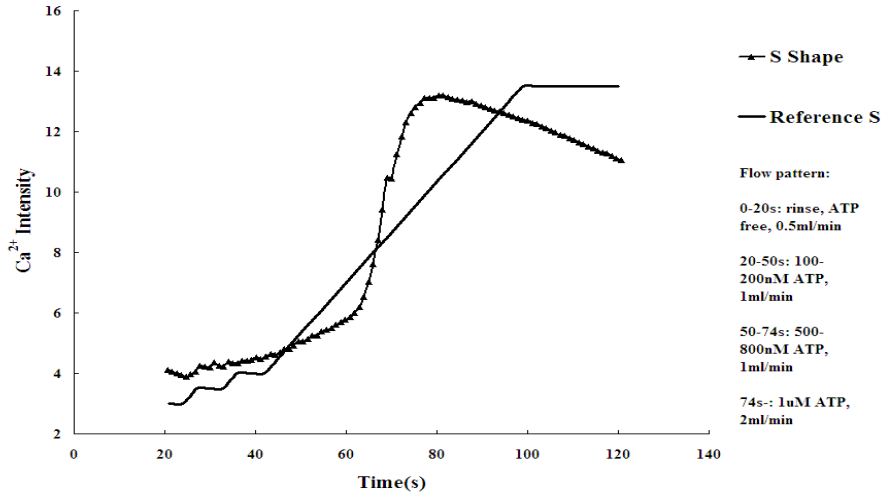

Figure 5.6: "S" shape. The bold solid line is the reference letter "S" and the line with triangles is the calcium intensity. HUVECs are rinsed gently with ATP free buffer at the flow rate of 0.5ml/min for 20 seconds. For the next 30 seconds, we increase ATP level by 100-200nM and flush the cells with a moderate flow rate (1ml/min). To generate a good "S" shape, the gradual but continuous increase of calcium level is necessary. We then elevate ATP level to 500-800nM for another 24 seconds while keep the flow rate as 1ml/min. In the last stage, ATP is added to 1μM and flow rate is adjusted to 2ml/min to maintain a relative high calcium level.

A distinguished feature in letter “S” lies in its middle part: a gradual but continuous increase. This indicates that stimuli should be exerted not too fast and intensive. That is why ATP level is elevated from 0, to 100, 500 and 1000nM in the end. It can seen from Fig 5.6 that the calcium intensity could not follow the reference “S” shape. It could not hold at a relative high level in the end.

The tracking performances shown in Fig 5.4-5.6 is a little bit far from satisfactory though they, to some extent, resemble these three letters. Besides measurement error and variation among individual tests, the open loop control strategy might also be considered to cause such tracking errors. Once the commands are set, we could not make any adjustment to the system according to its real time response. That brings us to the next section, where a feedback control strategy is utilized to facilitate the regulation of calcium level.

5.4.2 Closed Loop Control System

In the closed loop system, pictures taken by the CCD camera would be uploaded to the PC for further analysis. A set of fuzzy logic rules are built with which input signals could be updated. Here we would like to explain how the input signals are calculated. To plot letter “N”, for example, we first need a set of basal command, which is in fact the corresponding open loop command for “N”. If the tracking error falls within the tolerance, we would continue to use the basal command without any update. If the actual calcium intensity is larger than the reference, the controller would switch to “fast flow rate” and ”less ATP supplementation” mode. In our experiments, there are three kinds of tracking error (within tolerance, larger than upper bond and smaller than lower bond), three modes of flow rate (rapid, moderate and slow) and four different ATP levels (0, 200-500nM, 800-1000nM and 2μM). Commands sent to programmable syringe pumps would switch among these modes accordingly. Detailed closed-loop control schemes for generating letters “N”, “U” and “S” could be found in Appendix 1.

As can be seen from Fig 5.7, the calcium intensity could track quite close to the reference signal. However, the intensity is always lower than the reference when it stays in the higher level. Besides washing off the residual ATP, we have very limited means to decrease calcium level. That might explain why the tracking error is large after 100s.

Fig 5.8 demonstrates the system performance for tracking letter “U”. Compared with the open loop system shown in Fig 5.5, we can see the obvious improvement. This is mainly due to the fact that feedback information is used to help update commands.

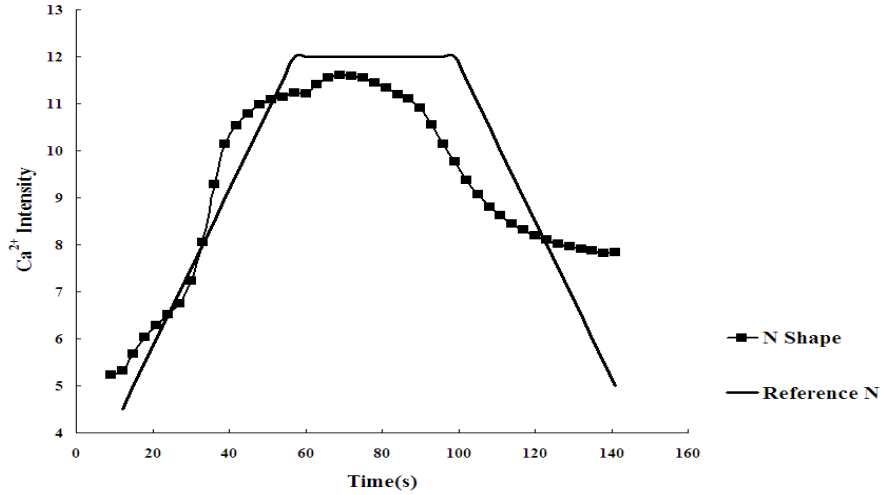

Figure 5.7: "N" shape generated via feedback control. The bold solid line is the reference letter "N" and the line with squares is the calcium intensity. HUVECs are rinsed gently with ATP free buffer at the flow rate of 0.5ml/min for 10 seconds. The picture is taken every 3 seconds and uploaded to the PC for further analysis. Input signals, i.e., the combination of different flow rate and ATP level are generated by an experience-based fuzzy rule.

Once the spike is detected, the control signal would switch to "slow" and "zero ATP" mode, which would reduce the tracking error dramatically.

We can also see similar improvements in generating letter "S" as displayed in Fig 5.9. The advantage of closed loop control is quite obvious in comparing the two sets of "NUS". Currently the control scheme relies a lot on experiences because the complete mathematical model for calcium dynamics has not yet been set up. This requires large amount of experimental data and we leave it as a future task.

5.5 Discussion

By adjusting the pumping rates of the two input syringes, we have obtained some simple patterns, which can always be triggered by the prescribed command signals. These results show that we could partially control intracellular calcium dynamics via shear stress and ATP. The monolayer of cells receive the input commands and make responses accordingly. It seems tougher to regulate these cells than to control the motion of DC motors. This might be due to the fact that we could only control the delivery of ATP onto VECs surface. Once ATP has arrived at the binding site, the

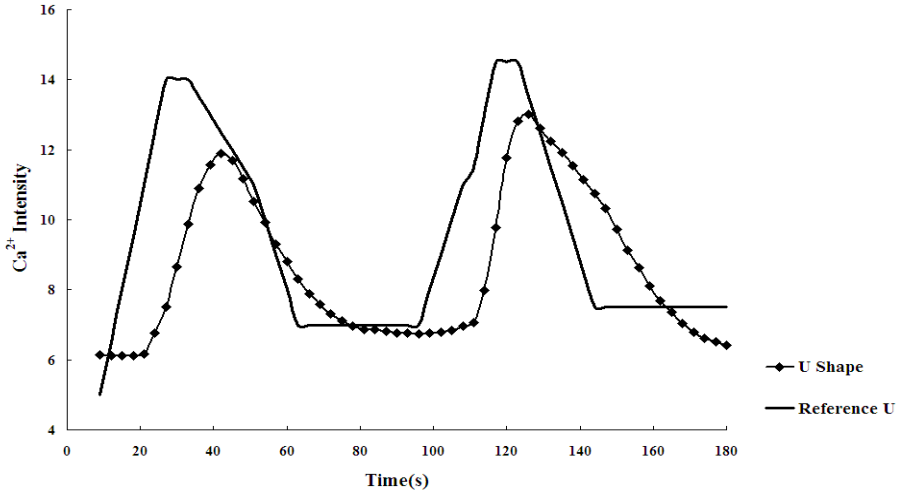

Figure 5.8: "U" shape generated via feedback control. The bold solid line is the reference letter "U" and the line with triangles is the calcium intensity. HUVECs are rinsed gently with ATP free buffer at the flow rate of 0.5ml/min for 10 seconds. The picture is taken every 3 seconds and uploaded to the PC for further analysis. Input signals, i.e., the combination of different flow rate and ATP level are generated by an experience-based fuzzy rule.

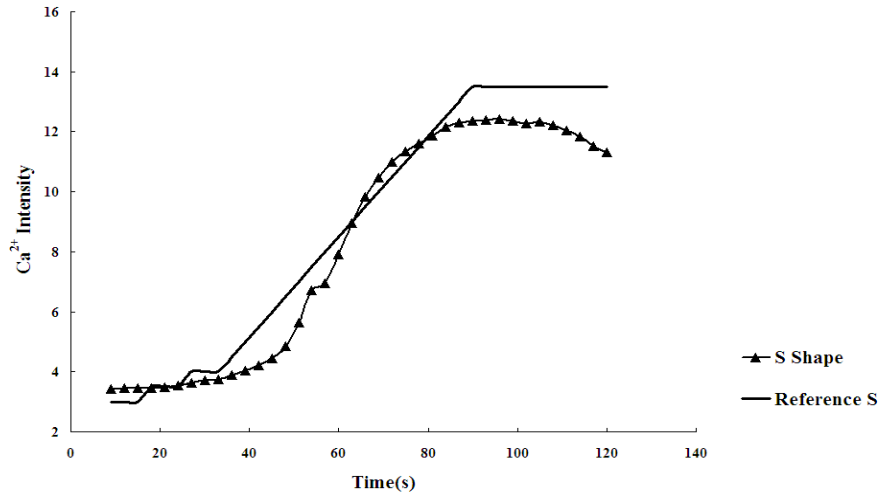

Figure 5.9: "S" shape generated via feedback control. The bold solid line is the reference letter "S" and the line with dots is the calcium intensity. HUVECs are rinsed gently with ATP free buffer at the flow rate of 0.5ml/min for 10 seconds. The picture is taken every 3 seconds and uploaded to the PC for further analysis. Input signals, i.e., the combination of different flow rate and ATP level are generated by an experience-based fuzzy rule.

downstream reactions would occur automatically, which is unfortunately out of our control. It is only the magnitude of shear stress and amount of endogenous ATP that are under relatively precise control. It has to be admitted that we are still far away from the inner structure of such biological plant and hence could not totally affect calcium response.

Measurement errors in cellular experiments are common. Different from the classical engineering plant, the measured features of a biological plant largely might vary a lot even the cells used are in the same passage. Therefore, we need to accept the fact that the precise tracking in DC motor may be to strict to VECs. Cells responses (i.e., ATP release amount or calcium level) are all acceptable in a physiologically reasonable range.

Specifications like fast response time, less overshoot and small tracking error are very common in controlling over a DC motor. However, shall we always follow these specifications when we face a biological plant? What kind of output is preferred? Does it make a lot of sense to pursue high precision? We believe it is problem dependent. What shall a desired response look like? It is better to ask biologists or physiologists who have a deeper understanding of the given problem.

Control over a biological plant (or even the behavior of a single cell) shares some features with those classical engineering plant. We can borrow some ideas from there and most of them are quite effective as proved by our own data. However, we should realize the differences between these two kinds of systems so that we could intervene the biological system and make it develop toward a beneficial direction.

Chapter 6

Conclusions

6.1 Summary of Major Contributions

The ultimate goal of our research work, as presented in this thesis, is to investigate the feasibility that the dynamics of intracellular calcium could be regulated via external mechanical/biochemical stimuli. As a large body of information for activating/terminating signaling pathways is encoded in the temporal/spatial pattern of calcium, adjusting its dynamics toward a prescribed profile would be of great benefit if a well correlation has been established between the profile itself and the corresponding physiological response downstream.

In this thesis, we focus on the "shear stress → ATP → calcium dynamics" signaling pathway, attempting to frame the mathematical structure of the pathway so that more detailed quantitative analysis could be conducted and what's more, control schemes could also be applied. As indicated by the thesis title, our research work covers device fabrication and cell experiments, mathematical modeling and controller design. Below summarizes the main contributions.

- **Experimentation**

    1. **Fabrication of perfusion/flow (PF) system**
       The PF system is a microfluidic device mimicking in vivo flow environment of blood vessel. The key procedure in fabrication is to generate the geometric pattern (150 microns in size) precisely. We have employed the photolithography technique to fulfill this task.
    2. **Construction of flow circuit**
       The flow circuit comprises two syringe pumps, one fluorescence microscope,

one CCD camera, one PC and PF system. The programmable pumps are used to generate different kinds of input signals to trigger the intracellular calcium response, which can be observed under microscope and captured by CCD camera for later analysis.

3. **Flow loading test**
   We have conducted flow loading tests for measuring shear-stress-induced ATP and intracellular calcium dynamics stimulated by shear stress and exogenous ATP. For measuring ATP, samples are taken directly from the outlet. We need one fluorescence microscope for calcium imaging.

- **Modeling**

  1. **Dynamic ATP release from VECs**
     We are the first to propose that shear-stress-induced ATP release from VECs has a strong dynamic feature. In all three dynamic models, the transient response of ATP release to time-varying shear stress is captured well.

  2. **Desensitization and reactivation**
     The proposed three dynamic ATP release models could all well capture the desensitization phenomenon, that is, cells tend to be adaptive to an unchanging stimulus and their responses become weaker. However these models bear different reactivation mechanisms. We finally verify that cells could be reactivated but with limited capacity via experiments. PID controller is also applied to regulate ATP level on VECs surface. Some satisfactory results are gained via simulation studies.

- **Control**

  1. **Open-loop Control Implementation**
     We have employed open-loop control strategy mostly based on experiences to explore whether intracellular calcium level could be affected by external stimulation. By adjusting shear stress and ATP level carefully, we finally generate letters “N”, “U” and “S”, representing National University.

  2. **Closed-loop Control Implementation**
     Some simulation results have been obtained on ATP release regulation via

PID controller. The results indicate that the ATP release amount could be controlled to some extent if with a delicate design of shear stress.
Feedback control based on fuzzy rules is also implemented to the regulation of intracellular calcium. The fuzzy rules for generating letters "N", "U" and "S" are developed on the basis of experiences and observations from open-loop control system. An improved system performance is finally gained.

6.2 Future Work

- **Toward more detailed investigations of related pathways**
  The more we understand a system, the better we could control over it. Facing such a complex biological system, we should put more time in understanding the mechanisms involved in the huge network. It is worthwhile to go deeper into the biological system and gain a full knowledge of what is happening there.

- **Toward more automatic and intelligent PF system**
  The PF system in current setup is a merely chamber where cells could settle down. Some other crucial procedures, like generating of dynamic flow pattern, mixing bio-chemicals at prescribed ratio and loading calcium indicator, are however manipulated externally, which enhances complexity in operation and also makes the whole setup cumbersome. In order to pack all these components into one single chip (match box size), micro-valves, mixers and power-supply unit should be integrated. What's more, a simple microprocessor is also needed to coordinate all parts to achieve the specifications.

- **Toward more humane control strategy**
  The most distinguishing feature in this thesis is that we have adopted a living plant, or to be more accurate, a batch of living cells as the objective and we wish to regulate/affect/control their behavior with limited understanding and knowledge of the cells. It is somewhat like nursing a kid and instructing him/her to behave in a manner beneficial to the community. However, the control strategy we have been now employing is a bit cold and in fact it is stemmed from our understanding of machines. Hence we think it necessary to develop more humane strategy, which of course is based on our deep understanding of the living system itself.

In summary, we have built a "living" plant and verified that the conventional engineering approach i.e., system and control theory is applicable to certain biological systems in cellular level. The major contributions of the work could be summarized from three aspects, that is mathematical modeling, experimentation and control implementation. We have contributed a dynamic ATP release model together with its updated versions to describe the desensitization and reactivation mechanism for membrane receptors. Furthermore, modeling the limited capacity of ATP release makes our model closer to the actual situation. The construction of the flow circuit for implementing fuzzy logic control considers to be the major contribution in experimentation. The fabrication of the perfusion/flow system is the foundation, without which the cellular experiments could not be accomplished in a more effective, economical and convenient fashion. Last but not least, we have explored the mysterious world of cell and have attempted to intervene its behavior via shear stress and exogenous ATP. Though the current work could hardly provide physiological or clinical implications regarding the effects brought about by the dynamic information encoded in intracellular calcium level, we still believe the successful regulation may hopefully open up a new scenario where control engineers are capable of optimizing the numerous biochemical reactions in living body.

Appendix 1: Control Schemes for Closed-Loop System

The closed-loop control signals, i.e., shear stress and ATP level, are generated under LabVIEW. Listed below are the three sets of fuzzy rules for generating letters "N", "U" and "S", respectively.

Fuzzy rule for letter "N"

```
Case 1: i <= 16
% hp: flow rate for pump 1 (no ATP);
% NE: flow rate for pump 2 (with high level ATP)
float32 hp; if (abs(error)<= 1.5) hp = 0.4; ne= 1-hp;
else if (error > 1.5) hp = 0.3; ne= 1-hp;
else hp = 0.5; ne= 1-hp;

Case 2: 17 <= i <= 25 float32 hp;
if (abs(error)<= 2.5) hp = 0.5; ne= 1-hp;
else if (error > 2.5) hp = 0.4; ne= 1-hp;
else hp = 0.7; ne= 1-hp;
```

```
Case 3: 26 <= i <= 37
float32 hp;
if (abs(error)<= 2.5) hp = 1.3; ne = 0.1;
else if (error > 2.5) hp = 1;ne = 0.1;
else hp = 1.5; ne = 0.1;

Case 4: 30 <= i <= 40
float32 ne;
if (abs(error)<=1.5) ne = 1.5; hp = 0.01
else if (error >1.5) ne = 1.8; hp = 0.01
else ne = 1; hp = 0.01;

Case 5: i >= 41
hp = 0.01; ne = 0.1;
```

Fuzzy rules for letter "U"

```
Case 1:1 <= i <= 9
float32 hp;
if (abs(error)<= 2.5) hp = 1; ne = 1.2-hp;
else if (error > 2.5) hp = 0.9; ne = 1.2-hp;
else hp = 1.15; ne =
1.2-hp;

Case 2: i=10
float32 hp;
```

```
if (abs(error)<= 2.5) hp = 0.8; ne = 1-hp;
else if (error > 2.5) hp = 0.6; ne = 1-hp;
else hp = 0.9; ne = 1-hp;

Case 3: 11 <= i <= 34
hp = 0.01; ne = 1-hp;

Case 4: 35 <= i <= 44
float32 hp;
if (abs(error)<= 2.5) hp = 1.5; ne = 0.1;
else if (error > 2.5) hp = 1; ne = 0.1;
else hp = 2; ne = 0.1;

Case 5: i = 45
float32 hp;
if (abs(error)<= 2.5) hp = 1.5; ne = 0.1;
else if (error > 2.5) hp = 1; ne = 0.1;
else hp = 2; ne = 0.1;

Case 6: 46 <= i <= 48
float32 ne;
if (abs(error)<=1.5) ne = 1; hp = 0.01;
else if (error >1.5) ne = 1.5; hp = 0.01;
else ne = 0.75; hp = 0.01;

Case 7: i>= 49
```

```
hp = 0.01; ne = 1;
```

Fuzzy rule for letter “S”

```
case 1: i <= 10
float32 hp;
if (abs(error)<= 2.5) hp = 0.2; ne = 1.2-hp;
else if (error > 2.5) hp = 0.1; ne = 1.2-hp;
else hp = 0.3; ne =
1.2-hp;

case 2: 11 <= i <= 19
float32 hp;
if (abs(error)<= 1.5) hp = 0.4; ne = 1- hp;
else if (error > 1.5) hp = 0.3; ne = 1- hp;
else hp = 0.5; ne = 1-
hp;

case 3: 20 <= i <= 25
float32 hp;
if (abs(error)<= 1.5) hp = 0.9; ne = 1.2-hp;
else if (error > 2.5) hp = 0.8; ne = 1.2-hp;
else hp = 1; ne =
1.2-hp;

case 4: 26 <= i <= 36
float32 hp;
```

```
if (abs(error)<=1.5) hp = 1.5; ne = 0.01;
else if (error >1.5) hp = 1.2; ne = 0.01;
else hp = 1.8; ne = 0.01;

case 5: i >= 37
hp = 0.01; ne = 1;
```

Appendix 2: Publication List

Journal Papers

1. K R. Qin, C. Xiang, Z. Xu, **L L. Cao**, S S. Ge and Z L. Jiang, "Dynamic modeling for shear stress induced ATP release from vascular endothelial cells", *Biomechanics and Modeing in Mechanobiology*, vol 7(5), pp. 345-353, 2008.

2. C. Xiang, **L L. Cao**, K R. Qin and T H. Lee, "Dynamic modeling and control of extracellular ATP concentration on vascular endothelial cells via shear stress modulation", *Journal of Control Theory and Application*, vol 7(1), pp. 123-129, 2009.

3. K R. Qin, C. Xiang and **L L. Cao**, "Dynamic modeling for flow-activated chloride-selective membrane current in vascular endothelial cells", *Biomechanics and Modeing in Mechanobiology*, vol 10(5),pp.743-754, 2010.

4. C. Xiang, **L L. Cao**, Q G. Wang and T H. Lee, "General framework for delay compensation for input-delay systems via predictive control design", *Control and Intelligent Systems*, vol 39(2), pp. 315-326, 2011.

Conference Papers

1. C. Xiang, **L L. Cao**, K R. Qin, Z. Xu and Ben M. Chen, "A modified dynamic model for shear stress induced ATP release from vascular endothelial cells", *International Conference on Life System Modeling and Simulation*, LNCS 4688, pp.462-272, 2007.

2. C. Xiang, **L L. Cao**, Q G. Wang and T H. Lee, "Design of predictor-based controllers for input-delay systems", *IEEE International Symposium on Industrial Electronics*, pp. 1009-1014, 2008.

References

Ando, J., Komatsuda, T. & Kamiya, A. (1988). Cytoplasmic calcium response to fluid shear stress in cultured vascular endothelial cells. *Vitro Cellular and Developmental Biology*, **24**, 871–877. 3, 12, 42

Ando, J., Ohtsukaa, A., Korenagaa, R. & Kamiya, A. (1991). Effect of extracellular ATP level on flow-induced Ca^{2+} response in cultured vascular endothelial cells. *Biochemical and Biophysical Research Communications*, **179**, 1192–1199. 42

Barakat, A.I. (2001). A model for shear stress-induced deformation of a flow sensor on the surface of vascular endothelial cells. *Journal of Theoretical Biology*, **210**, 221–236. 42

Berridge, M.J. (1997). The AM and FM of calcium signaling. *Nature*, **386**, 759–760. 54

Bodin, P. & Burnstock, G. (2001a). Evidence that release of adenosine triphosphate from endothelial cells during increased shear stress is vesicular. *Journal of Cardiovascular Pharmacology*, **38**, 900–908. 12, 18, 28, 29, 48

Bodin, P. & Burnstock, G. (2001b). Purinergic signalling: ATP release. *Neurochemical Research*, **26**, 959–969. 40, 42

Bodin, P., Bailey, B.J. & Burnstock., G. (1991). Increased flow-induced ATP release from isolated vascular endothelial but not smooth muscle cells. *British Journal of Pharmacology*, **103**, 1203–1205. 40

Chien, S. (2007). Mechanotransduction and endothelial cell hemeostasis: the wisdom of the cell. *American Journal of Physiology, Heart Circulation Physiology*, **292**, H1209–H1224. 1

Chiu, J.J. & Chien, S. (2011). Effects of disturbed flow on vascular endothelium: Pathophysiological basis and clinical perspectives. *Physiological Reviews*, **91**, 327–387. 1

Comerford, A., David, T. & Plank, M. (2006). Effects of arterial bifurcation geometry on nucleotide concentration at the endothelium. *Annals of Biomedical Engineering*, **34**, 605–617. 9

da Silva, C.G., Specht, A., Wegiel, B., Ferran, C. & Kaczmarek, E. (2009). Mechanism of purinergic activation of endothelial nitric oxide synthase in endothelial cells. *Circulation*, **119**, 871–879. 3

David, T. (2003). Wall shear stress modulation of ATP/ADP concentration at the endothelium. *Annals of Biomedical Engineering*, **31**, 1231–1237. 9, 12

Davies, P.F. (1995). Flow-mediated endothelial mechanotransduction. *Physiological Reviews*, **75**, 559–560. 1

Davies, P.F. (1997). Spatial relationships in early events of flow-mediated endothelial mechanotransduction. *Annual Review of Physiology*, **59**, 527–549. 1

Davies, P.F. (2009). Hemodynamic shear stress and the endothelium in cardiovascular pathophysiology. *Nature Clinical Practice*, **6**, 16–26. 1

Dolmetsch, R.E., Lewis, R.S., Goodnow, C.C. & Healy, J.I. (1997). Differential activation of transcription factors induced by Ca^{2+} response amplitude and duration. *Nature*, **386**, 855–858. 54

Dolmetsch, R.E., Xu, K. & Lewis, R.S. (1998). Calcium oscillations increase the efficiency and specificity of gene expression. *Nature*, **392**, 933–936. 54

Dudzinski, D.M. & Michel, T. (2007). Life history of eNOS: Partners and pathways. *Cardiovascular Research*, **75**, 247–260. 3

Dull, R.O. & Davies, P.F. (1991). Flow modulation of agonist(ATP)-response(Ca^{2+}) coupling in vascular endothelial cells. *American Journal of Physiology, Heart Circulation Physiology*, **261**, H149–H154. 3

Förstermann, U., Pollock, J.S., Schmidt, H.H., Heller, M. & Murad, F. (1991). Calmodulin-dependent endothelial-derived relaxing factor synthsase activity is present in the particulate and cytosolic fractions of bovine aortic endothelial cells.

Proceedings of the National Academy of Sciences of the United States of America, **88**, 1788–1792. 3

Fung, Y.C. (1981). *Biomechanics: Mechanical properties of living tissues*. Springer-Verlag. 42

Geiger, R.V., Berk, B.C., Alexander, R.W. & Nerem, R.M. (1992). Flow-induced calcium transients in single endothelial cells: Spatial and temporal analysis. *American Journal of Physiology, Cell Physiology*, **262**, C1411–C1417. 4

Grygorczyk, R. & Hanrahan, J.W. (1997). CFTR-independent ATP release from epithelial cells triggered by mechanical stimuli. *Amrican Journal of Physiology, Cell Physiology*, **272**, C1058–C1066. 12

Gu, X. & Spitzer, N.C. (1995). Distinct aspects of neuronal differentiation encoded by frequency of spontaneous Ca^{2+} transients. *Nature*, **375**, 784–787. 54

Guyot, A. & Hanrahan, J.W. (2002). ATP release from human airway epithelial cells studied using a capillary cell culture system. *Journal of Physiology*, **545**, 199–206. 9, 28

Hahn, C. & Schwartz, M.A. (2009). Mechanotransduction in vascular pysiology and atherogenesis. *Nature Reviews, Molecular Cell Biology*, **10**, 53–62. 1

Hallam, T.J. & Pearson, J.D. (1986). Exogeneous ATP raises cytoplasmic free calcium in Fura-2 loaded piglet aortic endothelial cells. *FEBS Letter*, **207**, 95–99. 3

Helmlinger, G., Berk, B.C. & Nerem, R.M. (1995). Calcium responses of endothelial cell monolayers subjected to pulsatile and steady laminar flow differ. *American Journal of Physiology, Cell Physiology*, **269**, C367–C375. 4

Ingber, D.E. (1991). Integrins as mechanochemical transducers. *Current Opnion in Cell Biology*, **3**, 841–848. 2

Ingber, D.E. (2003). Mechanobiology and diseases of mechanotransduction. *Annals of Medicine*, **35**, 1–14. 2

James, N.L., Harrison, D.G. & Nerem, R.M. (1995). Effects of shear on endothelial cell calcium in the presence and absence of ATP. *FASEB Journal*, **9**, 968–973. 4

John, K. & Barakat, A.I. (2001). Modulation of ATP/ADP concentration at the endothelial surface by shear stress: effect of flow-induced ATP release. *Annanls of Biomedical Engineering*, **29**, 740–751. x, 9, 11, 12, 15, 28, 44, 48, 49

Khakh, B.S. & North, R.A. (2006). P2X receptors as cell-surface ATP sensors in health and disease. *Nature*, **442**, 527–532. 40

Lagarias, J.C., Reeds, J.A., Wright, M.H. & Wright, P.E. (1998). Convergence properties of the nelder-mead simplex method in low dimensions. *SIAM Journal on Optimization*, **9**, 112–147. 16

Li, W., Llopis, J., Whitney, M., Zlokarnik, G. & Tsien, R.Y. (1998). Cell-permeant caged InsP3 ester shows that Ca^{2+} spike frequency can optimize gene expression. *Nature*, **392**, 936–941. 54

Lopez-Jaramillo, P., Gonzalez, M.C., Palmer, R.M. & Moncada, S. (1990). The crutial rule of physiological calcium concentrations in the production of endothelial nitric oxide and the control of vascular tone. *British Journal of Pharmacology*, **101**, 489–493. 3

Loscalzo, J. & Welch, G. (1995). Nitric oxide and its role in cardiovascular system. *Progress in Cardiovascular Diseases*, **38**, 87–104. 3

Malek, A. & Izumo, S. (1994). Molecular aspects of signal transduction of shear stress in the endothelial cells. *Journal of Hypertension*, **12**, 989–999. 4

Manz, A., Harrison, D.J., Verpoorte, E.M.J., Fettinger, J.C., Paulus, A., Lüdi, H. & Widmer, H.M. (1992). Planar chips technology for miniaturization and integration of separation techniques into monitoring systems: Capillary electrophoresis. *Journal of Chromatography A*, **593**, 253–258. 31

McDonald, J.C., Duffy, D.C., Anderson, J.R., Chiu, D.T., Wu, H., Schueller, O.J. & Whitesides, G.M. (2000). Fabrication of microfluidic systems in poly(dimethylsiloxane). *Electrophoresis*, **21**, 27–40. 31

Milner, P., Bodin, P., Loesch, A. & Burnstock, G. (1992). Increased shear-stress leads to differential release of endothelin and ATP from isolated endothelial cells from 4-month-old and 12-month-old male rabbit aorta. *Journal of Vascular Research*, **29**, 420–425. 40

Mo, M., Eskin, S.G. & Schilling, W.P. (1991). Flow-induced changes in Ca^{2+} signaling of vascular endothelial cells: Effect of shear stress and ATP. *American Journal of Physiology, Heart Circulation Physiology*, **260**, H1689–H1707. 3

Moncada, S. & Higgs, E.A. (2006). The discovery of NO and its role in vascular biology. *British Journal of Pharmacology*, **147**, S193–S201. 3

Nelder, J.A. & Mead, R. (1965). A simplex method for function minimization. *Computer Journal*, **7**, 308–313. 16

Nerem, R.M. (1992). Vascular fluid mechanics, the arterial wall and atherosclerosis. *Journal of Biomechanical Engineering*, **114**, 274–282. 1

Nocedal, J. & Wright, S.J. (1999). *Numerical Optimization*. Springer. 45

Nollert, M.U. & McIntire, L.V. (1992). Convective mass transfer effects on the intracellular calcium response of endothelial cells. *Journal of Biomechanical Engineering*, **114**, 274–282. 8

Nollert, M.U., Diamond, S.L. & McIntire, L.V. (1991). Hydrodynamic shear stress and mass transport modulation of endothelial cell metabolism. *Biotechnology and Bioengineering*, **38**, 588–602. 8

Ohura, N., Yamamoto, K., Ichioka, S., Sokabe, T., Nakatsuka, H., Baba, A., Shibata, M., Nakatsuka, T., Harii, K., Wada, Y., Kohro, T., Kodama, T. & Ando, J. (2003). Global analysis of shear-stress-responsive genes in vascular endothelial cells. *Journal of Atherosclerosis and Thrombosis*, **10**, 304–313. 2

Olsson, R.A. & Pearson, J.D. (1990). Cardiovascular purinoceptors. *Physiological Reviews*, **70**, 761–845. 3

Pirotton, S., Raspe, E., Demolle, D., Erneux, C. & Boeynaems, J.M. (1987). Involvement of inositol1,4,5-trisphosphate and calcium in the action of adenine nucleotides on aortic endothelial cells. *Journal of Biological Chemistry*, **262**, 17461–17466. 3

Plank, M.J., Wall, D.J. & David, T. (2006). Atherosclerosis and calcium signaling in endothelial cells. *Progress in Biophysics and Molecular Biology*, **91**, 287–313. 9

Ralevic, V. & Burnstock., G. (1998). Receptors for purines and pyrimidines. *Pharmacological Reviews*, **50**, 413–492. 40

Ranjan, V., Xiao, Z. & Diamond, S.L. (1995). Constitutive nitric oxide synthase protein and mRNA levels are elevated in cultured human and bovine endothelial cells exposed to fluid shear stress. *American Journal of Physiology, Heart Circulation Physiology*, **269**, H550–H555. 3

Rurchgott, R.F. & Zawadzki, J.V. (1980). The obligatory role of endothelial cells in relaxation of aterial smooth muscle by acetylcholine. *Nature*, **288**, 373–376. 3

Sabirov, R.Z. & Okada, Y. (2005). ATP release via anion channels. *Purinergic Signaling*, **1**, 311–328. 4

Sessa, W.C. (2005). Regulation of endothelial derived nitric oxide in health and disease. *Memórias Do Instituto Oswaldo Cruz, Rio De Janeiro*, **100**, 15–18. 3

Shen, J., Luscinskas, F.W., Connolly, A., Jr, C.F.D. & Jr, M.A.G. (1992). Fluid shear stress modulates cytosolic free calcium in vascular endothelial cells. *American Journal of Physiology, Cell Physiology*, **262**, C384–C390. 3

Shen, J., Jr, M.A.G., Luscinskasand, F.W. & Jr, C.F.D. (1993). Regulation of adenine nucleotide concentration at endothelium-fluid interface by viscous shear flow. *Biophysical Journal*, **64**, 1323–1330. 8

Sprague, R.S., Ellsworth, M.L., Stephenson, A.H., Kleinhenz, M.E. & Lonigro, A.J. (1998). Deformation-induced ATP release from red blood cells requires CFTR activity. *American Journal of Physiology, Heart Circulation Physiology*, **275**, H1726–H1732. 12

Toda, M., Yamamoto, K., Shimizu, N., Obi, S., Kumagaya, S., Igarashi, T., Kamiya, A. & Ando, J. (2008). Differential gene responses in endothelial cells exposed to a combination of shear stress and cyclic stretch. *Journal of Biotechnology*, **133**, 239–244. 2

Uchida, M.K. (1996). *Receptor Desensitization and Ca^{2+} signaling: cellular aspects of possible molecular dynamics*. Karger Press. 13

Virchow, R.L.K. (1850). *Cellular Pathology as Based Upon Physiological and Pathological Histology (translated from German)*. Philadelphia: J B. Lippincott. 1

Wan, J.D., Ristenpart, W.D. & Stone, H.A. (2008). Dynamics of shear-induced ATP release from red blood cells. *Proceedings of the National Academy of Sciences of the United States of America*, **105**, 16432–16437. 41

Whitesides, G.M. (2006). The origins and the future of microfluidics. *Nature*, **442**, 368–373. 31

Xiao, Z., Zhang, Z., Ranjan, V. & Diamond, S.L. (1997). Shear stress induction of endothelial nitric oxide synthase gene is calcium-dependent but not calcium-activated. *Journal of Cellular Biology*, **171**, 205–211. 3

Yamamoto, K., Korenaga, R., Kamiya, A. & Ando, J. (2000a). Fluid shear stress activates Ca^{2+} influx into human endothelial cell via P2X4 purinoceptors. *Circulation Research*, **87**, 385–391. 4

Yamamoto, K., Korenaga, R., Kamiya, A., Qi, Z., Sokabe, M. & Ando, J. (2000b). P2X4 receptors mediate atp-induced calcium influx in human vascular endothelial cells. *American Journal of Physiology, Heart Circulation Physiology*, **279**, H285–H292. 4, 15

Yamamoto, K., Sokabe, T., Ohura, N., Nakatsuka, H., Kamiya, A. & Ando, J. (2003). Endogenously released ATP mediates shear stress-induced Ca^{2+} influx into pulmonary artery endothelial cells. *American Journal of Physiology, Heart Circulation Physiology*, **285**, H793–H803. x, 4, 9, 12, 13, 14, 16, 22, 23, 24, 28, 29, 40, 41, 42, 43, 44

Yamamoto, K., Shimizu, N., Obi, S., Kumagaya, S., Taketani, Y., Kamiya, A., & Ando, J. (2007). Involvement of cell surface ATP synthase in flow-induced ATP release by vascular endothelial cells. *American Journal of Physiology, Heart Circulation Physiology*, **293**, H1646–H1653. 4, 12, 42